

Review

Earth-Abundant Electrocatalysts for Water Splitting: Current and Future Directions

Sami M. Ibn Shamsah 

Department of Mechanical Engineering, College of Engineering, University of Hafr Al Batin, P.O. Box 1803, Hafr Al Batin 31991, Saudi Arabia; sibnshamsah@uhb.edu.sa

Abstract: Of all the available resources given to mankind, the sunlight is perhaps the most abundant renewable energy resource, providing more than enough energy on earth to satisfy all the needs of humanity for several hundred years. Therefore, it is transient and sporadic that poses issues with how the energy can be harvested and processed when the sun does not shine. Scientists assume that electro/photoelectrochemical devices used for water splitting into hydrogen and oxygen may have one solution to solve this hindrance. Water electrolysis-generated hydrogen is an optimal energy carrier to store these forms of energy on scalable levels because the energy density is high, and no air pollution or toxic gas is released into the environment after combustion. However, in order to adopt these devices for readily use, they have to be low-cost for manufacturing and operation. It is thus crucial to develop electrocatalysts for water splitting based on low-cost and land-rich elements. In this review, I will summarize current advances in the synthesis of low-cost earth-abundant electrocatalysts for overall water splitting, with a particular focus on how to be linked with photoelectrocatalytic water splitting devices. The major obstacles that persist in designing these devices. The potential future developments in the production of efficient electrocatalysts for water electrolysis are also described.



Citation: Ibn Shamsah, S.M. Earth-Abundant Electrocatalysts for Water Splitting: Current and Future Directions. *Catalysts* **2021**, *11*, 429. <https://doi.org/10.3390/catal11040429>

Academic Editor: Rahat Javaid

Received: 23 February 2021
Accepted: 24 March 2021
Published: 27 March 2021

Publisher's Note: MDPI stays neutral with regard to jurisdictional claims in published maps and institutional affiliations.

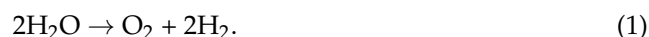


Copyright: © 2021 by the author. Licensee MDPI, Basel, Switzerland. This article is an open access article distributed under the terms and conditions of the Creative Commons Attribution (CC BY) license (<https://creativecommons.org/licenses/by/4.0/>).

Keywords: earth-abundant electrocatalysts; water splitting; hydrogen evolution reaction (HER); oxygen evolution reaction (OER); renewable energy

1. Introduction

Solar and other renewable energy sources are abundant and undependable. If our appetite for green energy increases, we will see a growing market for alternative energy storage devices in the future. The best way of using this energy is to use solar renewable energy to break water into hydrogen and oxygen, as shown in Equation (1) [1]. It is possible to store the hydrogen as a result of this reaction and work as green fuels. This would allow carbon-free energy and environmental protection.



Equation (1) requires $286.0 \text{ kJ mol}^{-1}$ of energy for a reaction at room temperature and pressure. Electrochemical methods tend to be very effective in producing hydrogen by only using electricity and water. Solar energy is the most effective renewable energy source (our Earth's surface received approximately $\sim 1.2 \times 10^{14} \text{ kJ}$ energy in every second) [2]. Based on the advances in the electrolytic process, there is a growing interest in coupling solar energy to the electrochemical water splitting process [3]. Thermodynamically, there are two ways of producing fuel from solar energy; the consumption of ordinary solar cells to operate conventional electrolyzers ("indirect" solar-to-hydrogen generation) or the creation of technologies that can absorb sunlight and split water at the same time ("direct" solar-to-hydrogen generation). Indirect techniques benefit from conventional methods by trail-and-tested technologies but are less successful due to additional steps needed. Electricity was first produced in the solar photovoltaic cell and then consumed by

electrolysis in an independent cell [4]. There has been a growing interest in developing and commercializing methods to generate solar-to-fuels efficiently in recent years [5,6]. This discovery of solar fuels would introduce the idea of “artificial photosynthesis,” where solar energy is absorbed and processed as a collection of chemical bonds converted into a solar fuel [7].

Figure 1 describes two separate solar-to-hydrogen photosynthesis mechanisms, in which the electrically active material is buried under the electrode and used as a cathode. Any realistic and scalable artificial photosynthesis systems would have strict material use criteria. The current densities from these devices would be restricted by the strength of the sunlight (0.1 Wcm^{-2}), meaning that factual, current densities are in the sequence of $10 \text{ mA}\cdot\text{cm}^{-2}$ for artificial photosynthesis systems in comparison with $\sim 0.5\text{--}2 \text{ Acm}^{-2}$ for commercial electrolyzers [8,9]. In order to generate the same quantity of gas per unit time, a solar energy to hydrogen photochemical smart device would need 50–200 times the electrode surface area of traditional electrical glass, rendering the use of precious metal electrocatalysts not economically feasible in such artificial photosynthesis systems. For artificial photosynthesis to work efficiently, catalysts must be cheaper and easily accessible to limit our choice to transition metals and their compounds in the first row [10]. Catalysts are also used for various applications such as renewable energy, biomass conversion, hydrogen production, efficient reactions in open and microreactor systems, etc. [11–35].

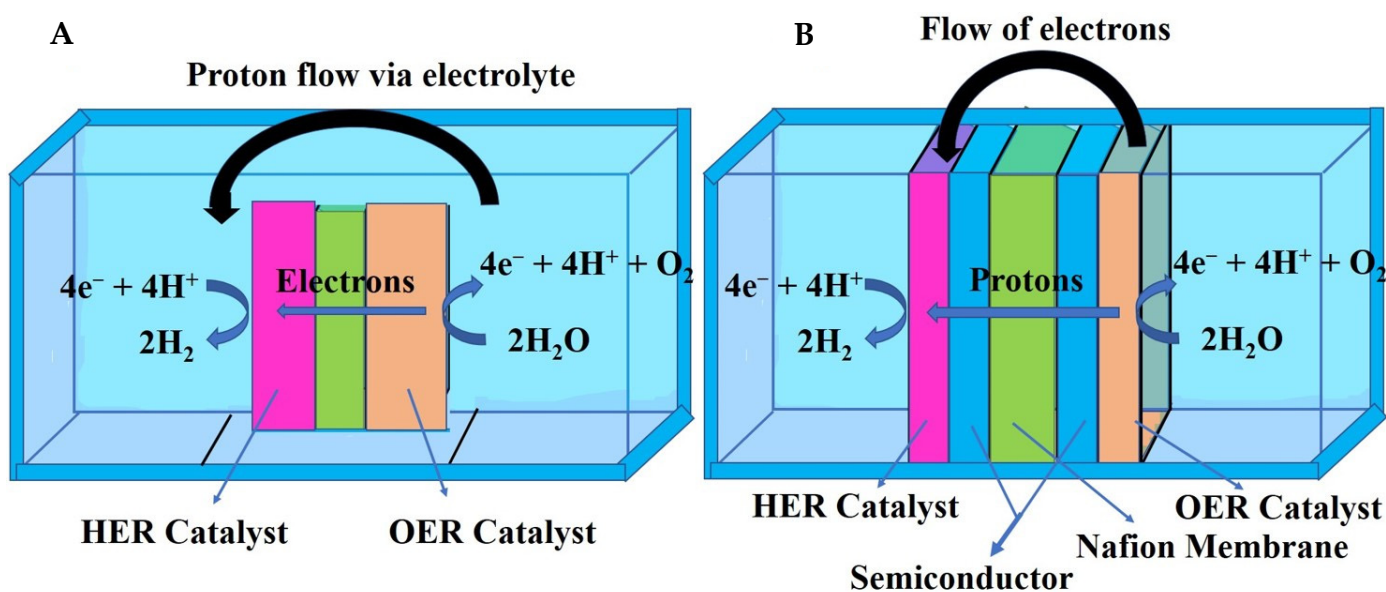


Figure 1. Artificial photosynthesis technology for solar energy into hydrogen processes: (A) wireless presentation and (B) wired configuration. Thus, it is preferable to use thinner catalyst layers in both situations. Adapted from [36].

Electrolysis works the best at a specific pH range, e.g., in acidic solutions or more alkaline media. However, the overwhelming majority of the semiconductors suitable for solar cells degrade at harsh pH values suggesting that developers are finding neutral electrolytes for artificial photosynthesis. In artificial photosynthesis systems, milder pH conditions can delay the rate of degradation of other cell components, which can be essential for more extended stability and total system cost [37]. In contrast, electrolyte solutions with neutral pH remove various safety hazards associated with utilizing extremely caustic electrolyte solutions. The appropriate electrolyte solutions will need to cover a large area to obtain usable fuel quantities on a reasonable timescale.

Herein, we have discussed recent developments towards the advancement of earth-abundant water splitting electrocatalysts in light for possible application in solar energy to hydrogen photoelectrochemical systems and the application of earth-abundant catalytic materials with and without Re, Ru, Pt, Ag, Os, Rh, Ir, Pd, and Au. We have also discussed the different forms of electrocatalysts for water splitting alongside descriptions of specific

catalytic materials in photoelectrochemical systems for the efficiency of the hydrogen evolution reaction (HER) and oxygen evolution reaction (OER). We demonstrate a complete and practical photoelectrochemical solar to hydrogen system and provide a crucial assessment of what remains to be accomplished in this area.

In acidic circumstances, oxidation occurs at the anode where water is oxidized, and this is called OER as shown in equation: (OER): $2\text{H}_2\text{O} \rightarrow \text{O}_2 + 4\text{e}^- + 4\text{H}^+$. The electrons pass through the external circuit, and protons reach the cathode to complete a circuit. The HER then takes place at the cathode, where protons and electrons combine to form hydrogen. (HER): $4\text{e}^- + 4\text{H}^+ \rightarrow 2\text{H}_2$. To enable the OER or HER to operate (water splitting), the theoretical potential voltage needs to be 1.23 V at room temperature. Even then, excessive energy is needed, allowing reactions to occur at adequate rates (activation energy). For a quicker water splitting rate (calculated as charge required per unit surface area for electrode per unit time and current density), the higher the activation energy required. The overpotential, often written as η , is the necessary voltage needed to reach a given current density. The main function of efficient electrocatalysts is to bring down the overpotential to an absolute minimum level. In basic circumstances, the HER and OER each follow these two equations



Based on earth-abundant electrocatalysis, Overall water splitting (OWS) is an outstanding technique used in the mass production of H_2 and O_2 fuel. Simple, activated earth-abundant materials can play essential roles as both active components and efficient support. In this case, two electrode systems not only are identical to commonly available electrocatalytic cells but also prevent the expensive use of Pt as a counter-electrode, with considerable electrocatalytic efficiency, and are durable against the OER and HER altogether in the same solution as fundamental specifications of such electrocatalysts. Considering the adsorption concept in strong electrocatalysts on the surface, there are three main pathways: electron, ion, and gases. Earth-abundant materials may also serve to encourage suitable OWS for industrial activity as a critical supporting material. Depending upon it, the research on OWS with both outstanding HER and OER efficiency using earth-abundant-based electrode materials is also desirable.

This paper aims to provide a concise review of the rapidly evolving research area for electrocatalysis. We hope this platform can prove beneficial to both beginners and those well enough in the topics under discussion [38,39]. Readers hoping for a more detailed recap on the electrocatalytic HER domains are guided elsewhere. Therefore, we will only research these heterogeneous catalysts that are readily available to replicate electrochemical devices (see Figure 1). We do not address homogenous or water scattering molecular structures, solely photocatalytic or systems in which HER or OER may only be accomplished through sacrificial reagents. Readers involved in these topics are highly encouraged to peruse different scholarly articles [40–42].

There are three significant classifications of water electrolysis, which vary based on the type of electrolyte, operating temperature, and ionic agents. The three primary electrolysis methods are proton exchange membrane electrolysis, alkaline electrolysis, and solid oxide electrolysis, as described in Figure 2 [43]. At present, alkaline electrolysis technology is commonly used on a commercial scale worldwide. However, it was discovered by Troost-wijk and Diemann in 1789 [44,45]. In this method, electrodes are dipped in basic KOH solution, and O_2 is generated at anode because of the oxidation process. In contrast, H_2 is collected at the cathode because of the reduction process (water splitting, Figure 2A [46,47]). First time in the 1980s, Donitz and Erdle documented solid electrolysis cell (SOEC). Still, this technology is unrefined, and more research work is needed for improvement. However, high hydrogen processing efficiency was exhibited in SOECs [48,49], and compelled the researchers to believe that there is an opportunity to be deployed commercially (Figure 2B).

Polymer membrane electrolysis was designed for space missions in 1960 to overcome the problems of alkaline electrolysis cells [50]. To extend this concept, solid sulfonated polystyrene-based membranes are introduced as an electrolyte and employed for water electrolysis in proton-exchange membrane fuel cells (PEMFCs) [50–53] (Figure 2C).

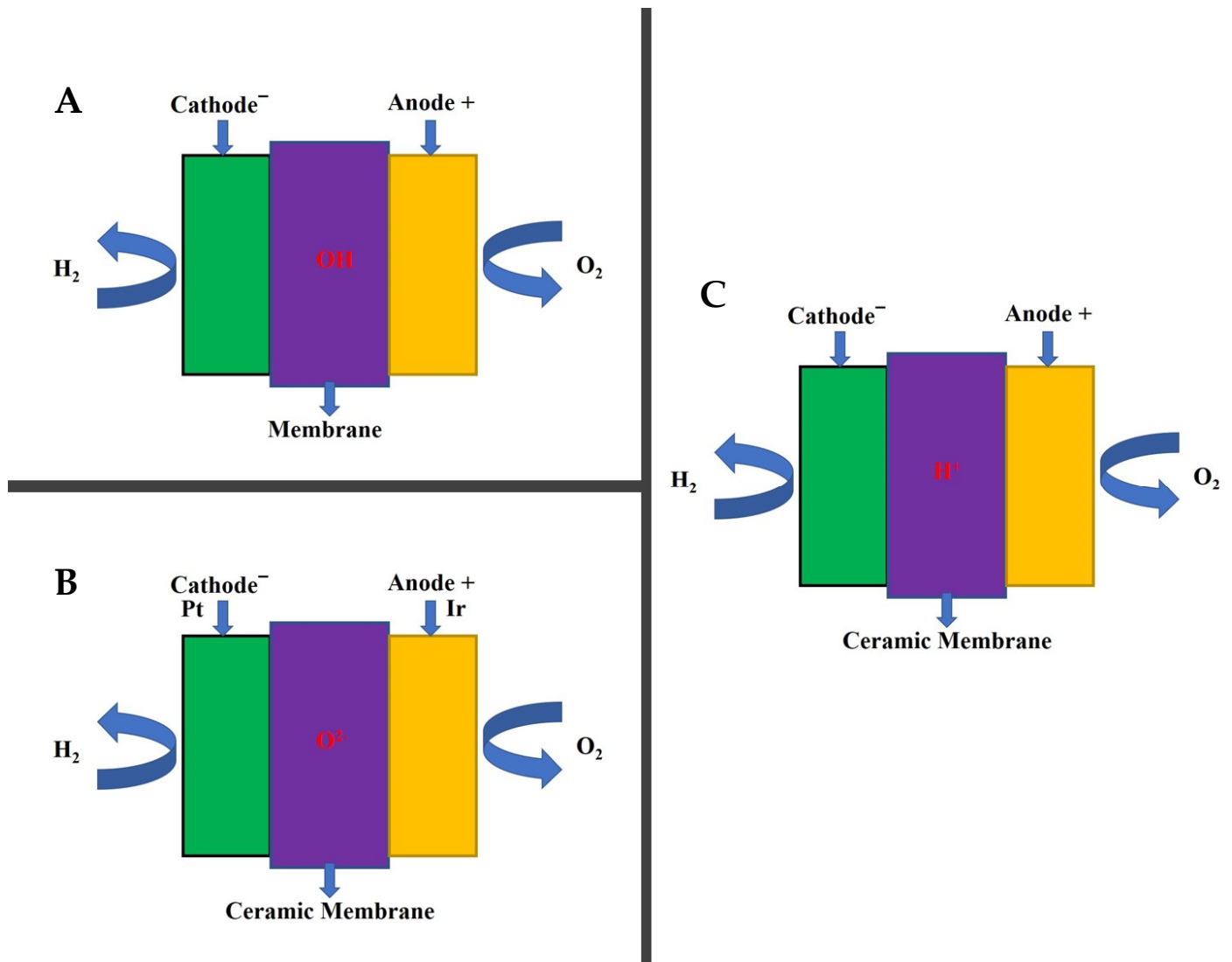


Figure 2. Schematic demonstration of (A) alkaline electrolysis, (B) solid oxide electrolysis, and (C) proton exchange membrane electrolysis. Reprint from [43]. Copyright (2021), with permission from Springer.

2. Evaluation of Electrocatalysts

There are two categories of electrodes used to test catalytic efficiency. One method of enhancing the nanostructured catalysts' properties (nanoparticles, nanosheets, etc.) is to coat on conductive surface content such as glassy carbon electrodes (GCE) or graphite paper. The other approach is to develop catalysts on a 3D structure like carbon fiber papers, Ni foam, Cu foam, or Ti mesh. 3D self-supported electrodes are stronger than 2D electrodes in terms of efficiency. They show better conductivity and surface and absence of paper binders, allowing ion or proton diffusion to occur quickly. We would pay much attention to 3D self-supported non-precious electrocatalysts since this is the first move towards commercial application [54–56].

For reliable estimation of the impact of HER or OER, specific relevant parameters need to be calculated or reported in the experiments, such as the overall/comprehensive catalytic activity, Tafel slope, exchange current density in terms of electron transportation, more

extended cycle stability, electrochemical impedance measurements, Faradaic performance, microcosmic parameter turnover frequency (TOF), and double-layer capacitance [57–59].

3. Earth-Abundant HER Electrocatalysts

Platinum (Pt) and palladium (Pd) as a heterogeneous catalyst for the HER are well-known for water electrolysis reaction at the cathode. However, the lack of noble metal-based catalysts is one of the main limitations for commercial applications [60,61]. To resolve this obstacle; investigators have managed to spread Pt-based catalysts on the surface of different substrates as supporting materials at the atomic level. Carbon black as support is another material widely used for dispersing Pt. There are two difficulties involved with the support technique. One challenge includes the unfavorable adjustment to the electronic and geometrical properties of Pt, and the other involves the potential disconnection of particles from the substrate, resulting in a dramatic drop in Pt catalytic activities [62–66]. In this case, carbon nanotube (CNT) are investigated and pledged to help additional treatments such as nitrogen doping for Pt-based nanoparticles (NPs) that can trigger the π electrons in the conjugated carbon. A group of researchers, Ma et al., fabricated a catalyst consisting of Pt-dependent nanoparticles anchored on CNTs of bamboos that showed a strong catalyst efficiency with an overpotential of 40 mV and an outline slope of 33 mV dec⁻¹. Such high catalytic performance of the catalyst was comparable with commercially available 20 wt% Pt/C electrocatalysts.

Until now, Pt-based catalysts have become the most powerful electrocatalysts for HER, but their large-scale industrial use has been hindered by low earth abundance and high prices. As a result, researchers are now concentrating on finding substitute materials used in water electrolysis as HER catalysts. Therefore, it has been a significant curiosity in hydrogen evolution electrocatalysts containing more earth-abundant elements. Nickel has been considered a critical HER catalyst for decades in strongly alkaline conditions (30% KOH in water). Hence, transition metal compounds, including nickel (Ni), cobalt (Co), and molybdenum (Mo) compounds (alloys, phosphides, sulfides, and nitrides), are of great significance as HER catalysts.

Agreeing with the Sabatier theory of electrocatalysis, the performance of the catalyst depends on the heat of the intermediate reaction absorption on the electrode surface [67]. For HER catalysts, the efficient performance is observed following a volcanic model in which the hydrogen binding energy is comparable to the state-of-the-art Pt catalysts (ΔG_H approximately zero). Incorporating other Ni metal products into alloys, like bimetallic NiCo, NiMo, NiCu, and ternary NiMoZn, is, therefore, the best suggesting way to manufacture electrocatalysts with improved HER performance. Furthermore, it is possible to observe synergetic effects by mixing two metals of transition, enhancing their electrical conductivity, and allowing Ni-Co alloys as an effective electrocatalyst due to rising intrinsic catalytic and corrosion resistance characteristics in a strongly alkaline aqueous environment [68–79].

It is helpful to consider different criteria used to measure the performance of a catalyst for OER or HER. Table 1 provides details about the overpotentials needed to achieve a defined current density and the Tafel slopes as possible descriptors compared to various catalysts based on electrochemical characterization. However, this is insufficient to conclude that current is responsible for generating gas. The reaction's outcomes must have been shown, and the substance's Faradaic yield should be calculated.

The so-called volcanic plates correlating the HER exchange densities with different materials using hydrogen chemisorption energy on these commodities are among the primary motivations behind the fabrication of new hydrogen evolution catalysts (Figure 3). Trasatti first reported this pattern for metals in the 1970s [80] and since then has become a productive treasure map for new catalysts [81,82]. This plot shows that the optimum catalytic activity is achieved for the highest potential hydrogen binding energy (hydrogen is not retained either too firmly or too weakly). Perhaps unexpectedly, this volcano has platinum at its apex.

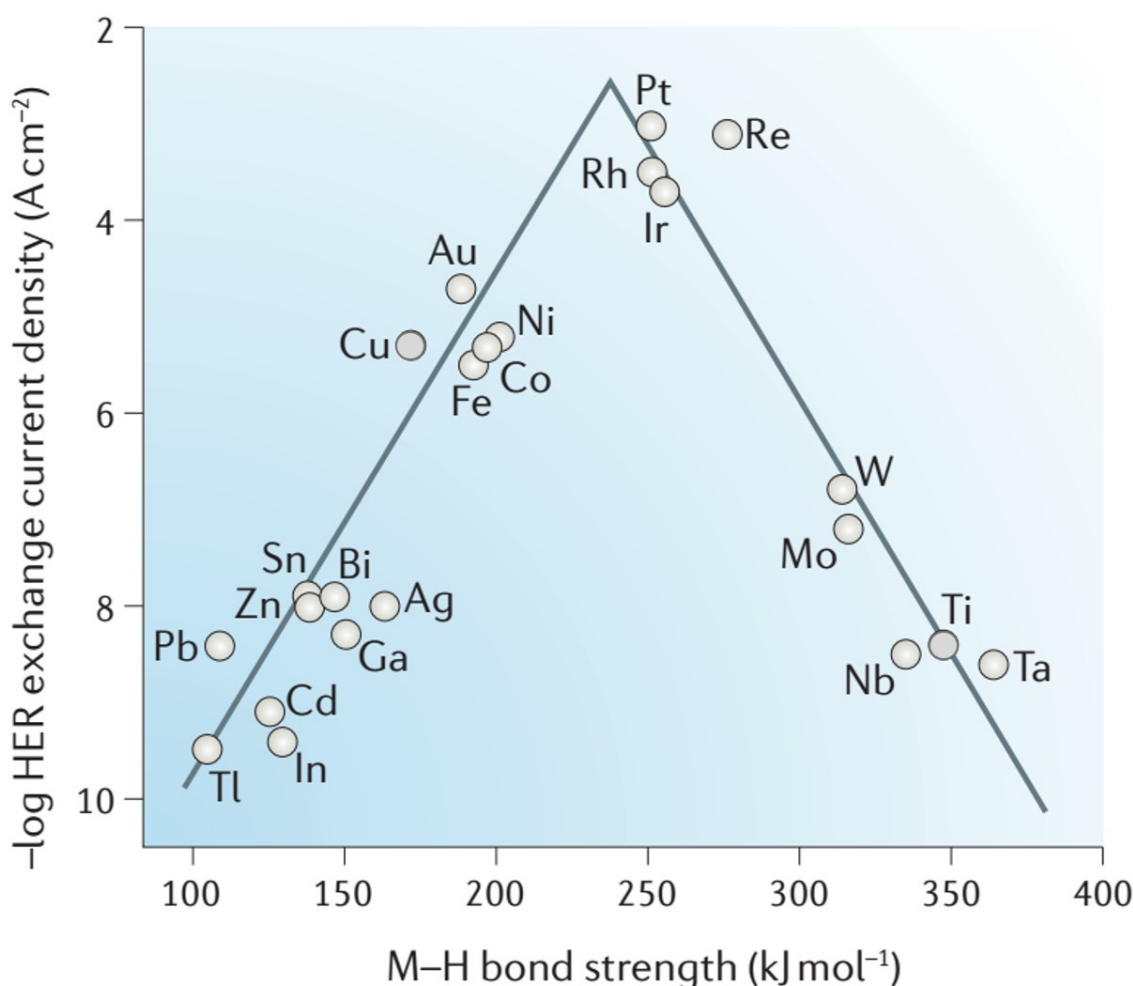


Figure 3. Trasatti's volcano plot for hydrogen evolution reaction (HER). The plot shows the exchange current densities for HER versus the metal–hydrogen bond strength when H adsorbed on the electrode surface. Reprint from [80]. Copyright (2021), with permission from Elsevier.

In 2005, Hinnemann and his colleagues used Density Functional Theory (DFT) to find a connection between atomic hydrogen binding to the catalyst surface and a material's free energy alteration [83]. Their findings indicated that MoS₂ would be a good alternative for HER, considering the fact that bulk MoS₂ is deemed to be a weak HER catalyst [84]. This apparent paradox was eventually clarified by some of the same group of scholars, who showed that the basal plane is much less involved than other edges [85,86]. Beginning with this finding, different transition metal sulfides and selenides have been synthesized by several methods (often to reveal as many active sites as possible) and shown to be capable of interacting with the HER [87–97].

Transition metal phosphides also have a role in HER catalysis. Popczun and colleagues observed that Ni₂P and MoS₂ are efficient hydrogen evolution catalysts in acidic media by acknowledging the Ni₂P and MoS₂ are typical hydrodesulfurization catalysts [98]. The common factor is that both hydrodesulfurization and HER involve reversible binding and cleavage of hydrogen. Phosphides have already been found to be efficient in several respects [99–101]. Researchers are progressively researching transition metal carbides, borides, and nitrides [102–105] because they work better in alkaline and acidic media [106–108]. Table 1 shows the electrocatalytic activity of earth-abundant transition metal-based compounds.

Table 1. The overview of the hydrogen evolution reaction (HER) performances of recently recorded electrocatalysts for water splitting.

Catalysts	Electrolytes	η for HER at j (mV@mA cm ⁻²)	Tafel Slope for HER (mV·dec ⁻¹)	References
NG@Co@Zn@ NF-850	1.0 M KOH	34@10	36	[109]
MoP@NPG	1.0 M KOH	126@10	56	[110]
Co ₂ P@N, P-CNTs	1.0 M KOH	132@10	103	[111]
NiN _x @porous carbon	1.0 M KOH	147@10	114	[112]
CoP@CNT	1.0 M KOH	67@10	54	[113]
MoS ₂ @N-CNTs	1.0 M KOH	110@10	40	[114]
CoP@BCN	1.0 M KOH	215@10	52	[115]
NC@CuCo Nitride	1.0 M KOH	105@10	76	[116]
Ni ₃ C@CNTs	1.0 M KOH	132@10	49	[117]
Fe ₃ C@Mo ₂ C@N-C	1.0 M KOH	116@10	43	[118]
NC@Vo-WON	1.0 M KOH	16@10	33	[119]
Mo/Co@N-C	1.0 M KOH	157@10	148	[120]
Ni ₃ N@CQD	1.0 M KOH	69@10	108	[121]
Ni-Cr@CF	1.0 M KOH	144@10	88	[122]
N-Mo ₂ C	1.0 M KOH	52@10	50	[123]
MoP NA/CC	1.0 M KOH	124@10	58	[124]
MoS ₂ /C ₃ N ₄	1.0 M KOH	153@10	43	[125]
Co ₉ S ₈ -NiS	1.0 M KOH	163@10	83	[126]
Co ₂ P NRs	1.0 M KOH	45@10	67	[127]
NiS/MoS/C	1.0 M KOH	117@10	58	[128]
Ni/Co-NC	1.0 M KOH	68@10	180	[78]
MoS _x @NiO	1.0 M KOH	406@10	43	[129]
Co-MoS ₂	1.0 M KOH	203@10	158	[130]
MoS ₂ /NiCo-LDH	1.0 M KOH	78@10	77	[131]
MoS ₂ /NiS/MoO ₃	1.0 M KOH	91@10	55	[132]
MoSe ₂	1.0 M KOH	310@10	93	[133]
CoSe ₂ /MoSe ₂	1.0 M KOH	218@10	76	[134]
Ni(OH) ₂ /MoS ₂	1.0 M KOH	227@10	105	[135]
Ni ₃ S ₂ /NF	1.0 M KOH	296@10	65	[136]
Mo-NiCoP	1.0 M KOH	269@10	77	[137]
EBP@NG	1.0 M KOH	265@10	89	[138]

Another group of researchers [139], prepared an excellent electrocatalyst for HER using a nickel metal-organic framework at 700 °C; as a result of the carbonization process, carbon nanoparticles were synthesized with dispersed Ni atoms. This prepared electrocatalytic material's performance showed better for HER at strong acidic media with pH nearly equal to 0. Catalysts that are anticipated on comparatively little atomic clusters are often responsible for fast degradation under continued potential due to metal particulates agglomeration. However, in this scenario, the catalysts continuously worked for more than 25 h, which is a noteworthy conclusion. The volcanic plot's challenge enables efficient HER catalysts to be suggested in designing new materials with variable hydrogen energy binding by combining the catalysts on opposite slopes of the volcano. Lu and his

colleagues [140] have applied this method along with DFT calculations to estimate that Cu substrate working as support with doping of titanium indicated that hydrogen binding energies were comparable to platinum. Therefore, the team of researchers synthesized a series of Cu-Ti-based bimetallic films adopting an arc-melting process and evaluated their performance in alkaline media (0.1 M KOH). The highest HER performance was achieved with $\text{Cu}_{95}\text{Ti}_5$ films, which provided current densities of $-10 \text{ mA}\cdot\text{cm}^{-2}$ only with an overpotential of 60 mV. In contrast, available commercial Pt/C catalyst to attain the same current density, an overpotential of 100 mV is necessary, implying that earth-abundant HER catalysts under some circumstances will outcompete platinum.

More recently, Qazi et al. successfully employed surface-modified copper foam along with Ni-Cr-based transition metals and used it for superior HER performance electrode material, as shown in Figure 4. The corresponding Ni-Cr@CF demonstrates a high electrocatalytic performance towards HER and achieved 10 mA cm^{-2} current density with 144 mV overpotential and Tafel slope value of 88 mV dec^{-1} , in 1.0 M KOH strong alkaline media. As-prepared bimetallic Ni-Cr on the Cu-foam substrate (CF) verified the strong association between the active sites and the supporting material, which guaranteed the efficiency improvements of the charge transport and quick reaction kinetics as well as their stability even after 2000 cycles. The principle of surface modification of conductive CF substrate with an effective combination of low-cost earth-abundant transition metals as a catalytic material supports achieving high-performance HER electrocatalysts. The main obstacle for developing low-cost, efficient HER electrocatalysts is demonstrating that the activity should be sustained longer time [122].

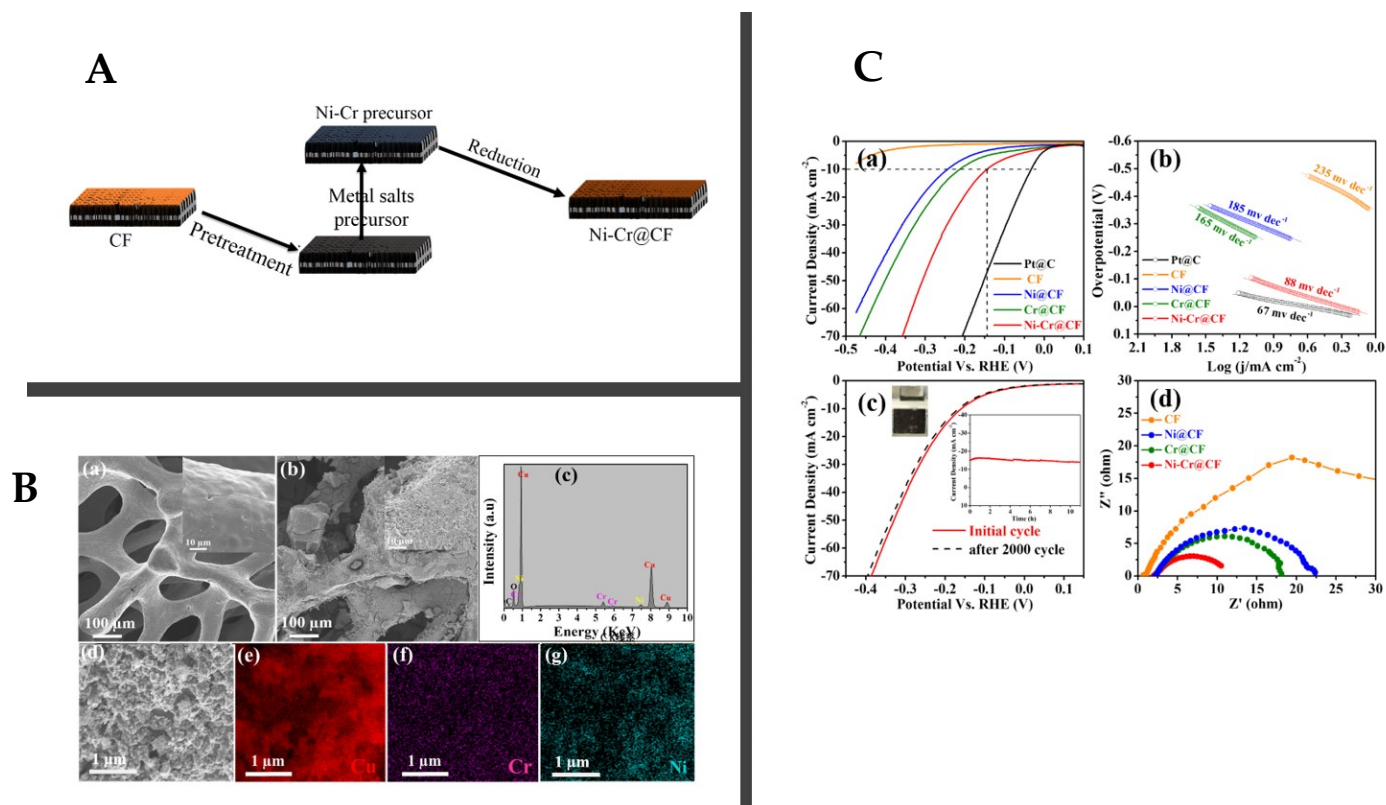


Figure 4. (A) Schematic illustration for the surface-modified Ni–Cr@CF, (B) corresponding SEM images (a,b) and elemental mapping of the selected area (c–g), (C) Prepared Ni–Cr@CF electrocatalyst with efficient HER performance, Tafel slope, stability test and Electrochemical impedance spectra (EIS) respectively (a–d). Reprint from [122]. Copyright (2021), with permission from Elsevier.

4. Earth-Abundant OER Electrocatalysts

Apart from HER, the other water splitting half-reaction is OER. Merrill and Dougherty [141] observed NiFe oxide on Pt as support that needs only 30 mV overpotential to conduct the OER at 1 mA cm^{-2} in strong alkaline media (pH 14). Some other groups and their colleagues have also recorded healthy OER practices for NiFe oxides in alkaline media [142]. The results demonstrated in this work that a small number of iron loadings showed improvement in OER. However, higher amounts acted to minimize efficiency in comparison to nickel oxides without other metals doping. The Corrigan work presented in the 1980s [143] previously confirmed the claim that there was a substantial rise in the electrocatalysis of OER when the iron is doped at a lower level as 0.01% in nickel oxide. Some other researchers [144] have also discussed the impact on OER performance when Fe was doped on a nickel oxide substrate. They observed the best OER performance with an optimum composition of Fe:Ni that is 2:3 [145,146].

Bell and co-workers investigated the influence of iron doping on the OER behavior of nickel oxides in-depth [144]. They also observed that NiFe oxide OER operation is optimum at a Fe:Ni composition of 2:3. The authors proposed that the rise in potential was observed in the region where the OER was done due to the oxidation process of Ni(ii) to Ni(iii). However, the Fe(iii) centers present in these films need less overpotential for OER than Ni(iii) centers. In contrast, Fe(iii) centers have been regarded as active sites for oxygen production/evolution. Nickel and iron seem to be advantageous when developing high-performance active catalysts for OER under alkaline media [147,148]. Table 2 indicates that the leading OER catalysts are based on these two metals. Another group of researchers delivered a significant outcome in this field with substantial consequences in electrochemical water splitting at high pH [149,150] using Ni-salt precursor for synthesizing Ni-oxide and found Fe traces in as-prepared active material. It was also noticed that the overpotential for OER changed from 300 to 470 mV when Fe traces were removed from the active material. The appropriate efficiency of OER was found at 25% Fe doping on Ni-oxide substrate films. Similar effects were observed with Fe doping on cobalt oxide material [151]. A study demonstrated in several widely used electrolytes (such as phosphate, carbonate, or borate salts) that adventitious nickel could induce current OER densities of 1 mA cm^{-2} at just 400 mV overpotential even though no known catalyst were present. It could also be more troubling for those who worked in this field [152].

Xu and his co-workers reported highly efficient electrocatalyst based on Bimetallic phosphide hollow nanocubes synthesized from metal-organic frameworks (MOF). The as-prepared catalyst worked efficiently for OER. Hence, pointed out again that the fabrication of cost-effective, efficient, and durable catalysts based on Earth-abundant materials are critical for water splitting. The researchers employed a basic phosphorylation technique using MOF (Ni-Fe Prussian blue analog) as a template for novel bimetallic phosphide hollow nanostructures ((Ni_{0.62}Fe_{0.38})₂P₃; Figure 5). The final product demonstrated a perfectly prepared hollow cubic structure with more surface area for reaction kinetics and synergistic effects due to the bimetallic interactions for electron transportation support towards enhancing the excellent activity of OER in extreme alkaline media with low onset potential, small Tafel slope, and good stability. Only 290 mV overpotential was needed to reach the current density of 10 mA cm^{-2} , which is even more efficient for OER than monometallic phosphide Ni-P or Fe-P catalysts as well as the commercially available IrO₂ catalyst [153].

Table 2. The overview of the oxygen evolution reaction (OER) performances of recently recorded electrocatalysts for water splitting.

Catalysts	Electrolytes	η for OER at j ($\text{mV}@\text{mA cm}^{-2}$)	Tafel Slope for OER ($\text{mV}\cdot\text{dec}^{-1}$)	References
(Ni _{0.62} Fe _{0.38})P	1.0 M KOH	290@10	44	[153]
FeNi _{4.34} @FeNi	1.0 M KOH	283@10	53	[154]
NiCo ₂ O ₄ /Ti	1.0 M KOH	353@10	61	[155]
(3D) CoP@CoFe-LDH	1.0 M KOH	240@40	69.2	[156]
Co-C@NiFe LDH	1.0 M KOH	249@10	58	[157]
NiO _x NCs	1.0 M KOH	330@10	105	[158]
Co ₃ O ₄ nanosheet	1.0 M KOH	367@10	65	[159]
NiFe ₂ O ₄ /rGO	1.0 M KOH	302@10	63	[160]
0.3 TA ⁻ Co/Fe-C	1.0 M KOH	284@10	86	[161]
CoCrFeNiMo HEAs	1.0 M KOH	220@10	59	[162]
MnFe ₂ O ₄ /NF	1.0 M KOH	310@10	65	[163]
Fe-NiCoP/PBA HNCs	1.0 M KOH	290@10	70	[164]
MoSe ₂ -CoSe ₂ /CoAl-LDH	1.0 M KOH	320@10	71	[165]
(NiFe-PBA)-F	1.0 M KOH	190@10	57	[166]
Co@PTh	1.0 M KOH	338@10	52	[167]
CeO ₂ /NiFe-LDH	1.0 M KOH	246@10	67	[168]
Fe-CoNi-OH//CoP	1.0 M KOH	210@10	28	[169]
CoP ₂ /Fe-CoP ₂ YSB	1.0 M KOH	266@10	68	[170]
Se-(CoFe)S ₂	1.0 M KOH	281@10	52	[171]
Ni _{0.4} Fe _{0.6} Te ₂ /NF	1.0 M KOH	190@10	26	[172]
MOF-V-Ni ₃ S ₂ /NF	1.0 M KOH	268@10	99	[173]
Fe-Ni ₃ S ₂ /FeNi	1.0 M KOH	282@10	54	[174]
Ni ₃ N-NiMoN	1.0 M KOH	277@10	118	[175]
Ni ₃ N-NiMoN	1.0 M KOH	198@10	42	[176]
NF@Fe ₂ -Ni ₂ P/C	1.0 M KOH	205@10	52	[177]
CoP ₂ /RGO	1.0 M KOH	300@10	96	[178]
Co-Ni-Se/C/NF	1.0 M KOH	275@10	63	[179]
MoS ₂ /NiS ₂	1.0 M KOH	278@10	92	[180]
MoS ₂ /NiS	1.0 M KOH	370@10	108	[181]
Ni ₃ S ₂ /NF	1.0 M KOH	296@10	65	[136]
MoSe ₂ /MXene	1.0 M KOH	340@10	90	[182]

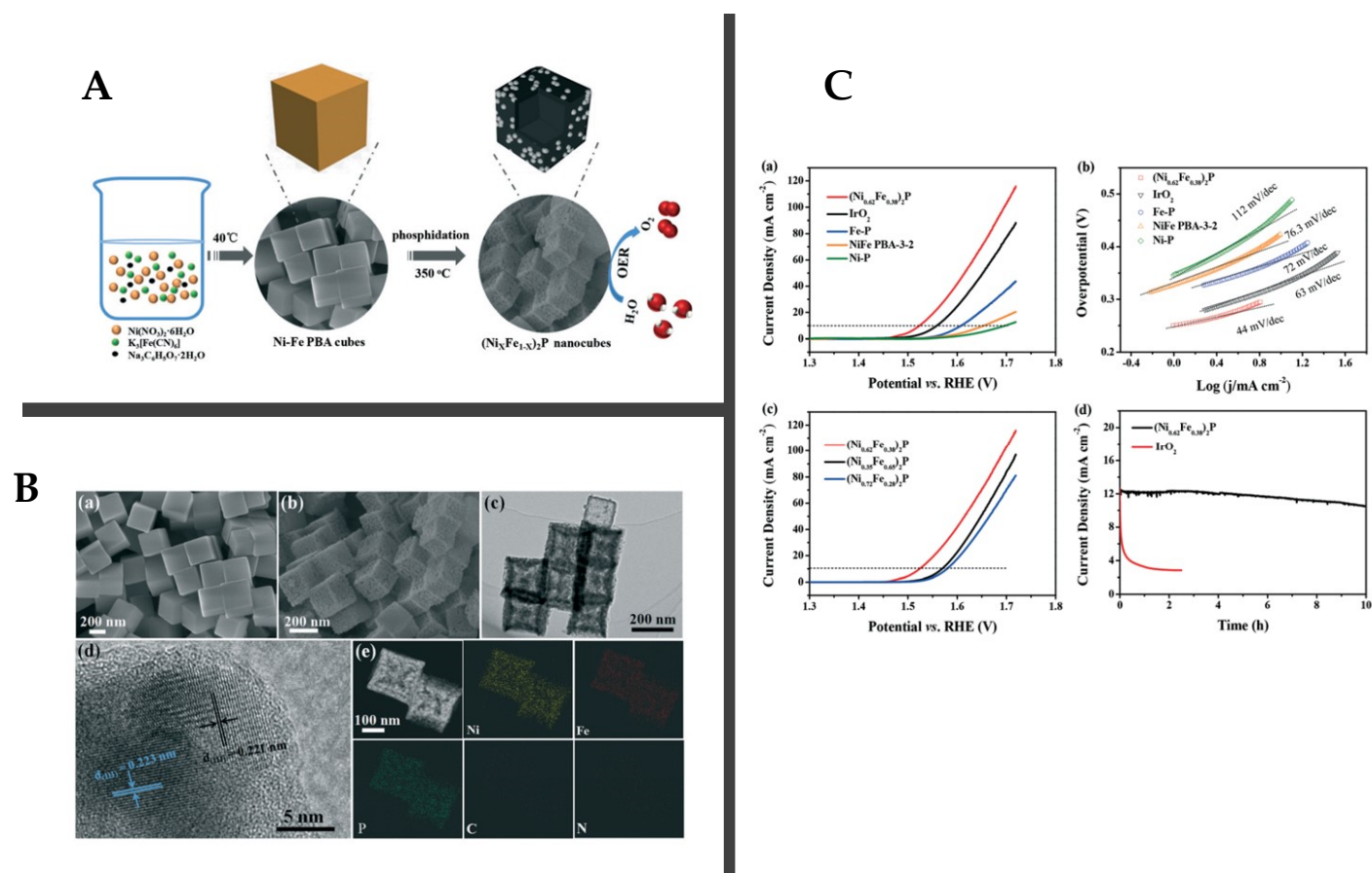


Figure 5. (A) Schematic illustration for preparation method, (B) corresponding TEM images (a–c), HTERM (d) and elemental mapping of the selected area (e) to describe the morphology, (C) as-prepared electrocatalyst with efficient oxygen evolution reaction (OER) performance (a), Tafel slope (b), and stability tests (c,d) respectively. Reprint from [153]. Copyright (2021), with permission from RSC.

Other than the MOF-based materials, the same group of researchers (Qazi et al., 2017) explained a simple, facile method for the preparation of bimetallic $\text{FeNi}_{4.34}$ NPs directly anchored on FeNi-foil substrate ($\text{FeNi}_{4.34}@\text{FeNi}$) as high-performance OER electrode material. $\text{FeNi}_{4.34}@\text{FeNi}$ electrode exhibits superior activity for OER in an intense 1.0 M KOH solution. A lower overpotential of 283 mV was obtained to achieve a current density of 10 mA cm^{-2} with a small Tafel slope value of 53 mV dec^{-1} . It confirmed the formation of small FeNi particles on the surface of FeNi-foil substrate that supports the fast electron transport to enhance significant electrocatalytic OER activity and durability [154].

For the first time, bimetallic Fe-Ni sulfide nanosheets formation on FeNi alloy marked as $\text{Fe-Ni}_3\text{S}_2/\text{FeNi}$ was reported by Yuan et al. as an optimized OER electrode material. The fundamental source and hypothesis of improved OER operation were discovered with the theoretical calculation using DFT and results obtained from experiments. The as-prepared electrode shown a strong catalytic and longer time durability in harsh alkaline media with overpotential as low as 282 mV at 10 mA cm^{-2} and 54 mV dec^{-1} Tafel slope value. When the exemplary behavior and robust properties were integrated, it indicated that the electrode in the as-prepared state gives an appealing alternative to noble metal-based catalysts. The excellent OER efficiency could be explored and explained in terms of the efficient electron transportation ability, presence of a higher number of active sites with appropriate OER reaction kinetics, and energetic incorporation of doped Fe species. This research not only produces an exceptional electrode for water oxidation but also leads into considerable detail on the mechanisms of enhanced OER efficiency that can prove to be a reference in the creation of robust and integrated OER electrodes (Figure 6) [174].

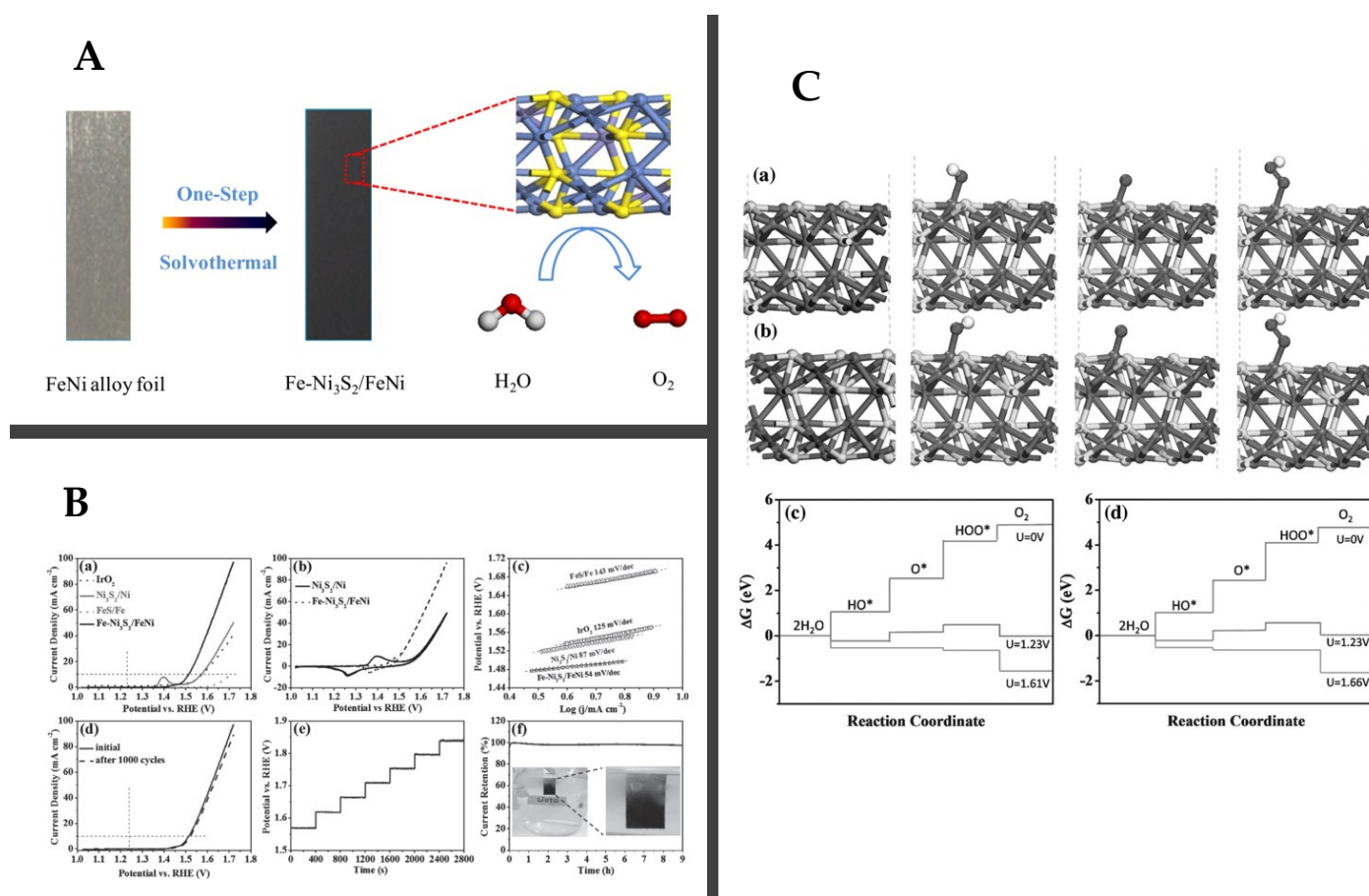


Figure 6. (A) Schematic illustration for preparation method, (B) Prepared electrocatalyst Fe–Ni₃S₂/FeNi with efficient OER performance (a,b), Tafel slope (c), stability test (d), Time-dependent current density curves (e) and the corresponding photographs of water oxidation device (f), (C) Density Functional Theory (DFT) calculations in Scheme (a–d) Reprint from [174]. Copyright (2021), with permission from Wiley.

5. Summary, Challenges, and Future

5.1. Summary

Water electrolysis is an emergent research area for power storage and conversion, known as an essential method for synthesizing hydrogen and pure oxygen. Alkaline and polymer electrolyte membrane (PEM) electrolysis are currently considered advanced, although solid oxide electrolyzer cell (SOEC) is still in the laboratory. In order to increase the energy efficiency of water electrolysis, both HER and OER, the two requisite reactions must be enhanced kinetically. Noble metals are considered the best electrocatalysts in this area. However, the marketing of water electrolysis technology is hampered by similar problems, such as high prices and poor availability of noble metals. While changes have been made to minimize noble metal loading by altering the compositions and morphologies of materials or replacing non-noble metal-based catalysts with a noble metal, substantial progress has been inadequate.

Due to the comprehensive analysis of transitional metal compounds, such as Ni, Co, Mn, and Fe compounds and their oxides (MO_x), phosphides (MP_x), sulfides (MS_x), and alloys (MM''), noble metal catalysts have been substituted by water electrolysis in recent years for both OER and HER. Catalytic improvement has been accomplished here using many different methods, including improving electrical conductivity by alloying, increasing stability and conductivity through synthesizing bimetallic compounds, and generating synergistic effects through combining naturally conducting carbon with chemical-reactive metallic hybrid compounds. Furthermore, literature has thoroughly explored the impact of

morphology on electrocatalytic efficiency adopted models for template-free and template-assisted fabrication techniques. In addition, the position of electrodes has also been investigated by the use of different substrates, including carbon cloth, graphite carbon, carbon black, copper foam (CF), and nickel foam (NF), for increasing catalyst efficiency. Materials such as NF and CF, which have shown long-range porous structures and enable charge transport and mass transfer, can be used as platforms for designing promising 3D materials as a self-supported electrode.

For PEM electrolysis, non-noble metal catalysts with efficient efficiency have not yet been clearly identified concerning longer stability. Because the electrolysis procedures involved the use of acids with very high concentrations that are highly corrosive to most metals, and a limited number of non-noble metal catalysts can bear strong acidic electrolytes in the PEM electrolysis process. While the pure, noble metals are not ideal as catalysts for OER because of high cost and scarcity, they may be combined with other non-noble metals or doped at support material during the time of synthesis. Non-precious metal oxides and carbides, namely, niobium oxide (Nb_2O_5), tin oxides (SnO_2), tantalum oxide (Ta_2O_5), titanium oxide (TiO_2), tungsten carbide (WC), and TiC, may be used as electrodes for reducing the noble loading of the metal and for reducing total operating expense. For PEM electrolysis, noble metals are still required since the substitution of noble metals with non-noble metal catalysts for OER remains challenging to achieve. This means that more durable electrocatalysts based on non-noble metals, such as Fe-N-C and Co-N-C, should be developed and established. Many of the catalysts used for OER and HER processes running at high temperatures are not stable, especially for SOECs. The active electrode surface must be expanded, and three significant variables, including ion conductivity, electrical conductivity, and catalytic activity, should be explored.

Extensive research on water electrolyzing technology was conducted on HER and OER with noble metal and non-noble metal-based catalysts. Though the studies have provided many innovative ideas for developing robust, cost-effective, and reliable catalysts for water electrolysis in various systems, there are still numerous technical difficulties, which are examined as follows.

5.2. Challenges in Electrocatalysts for Water Splitting

In recent years, the high cost of noble metal catalysts has led to a thorough investigation of non-noble metal catalysts for both OER and HER methods to minimize or eliminate the use of noble metal. However, the development of low-cost non-noble electrocatalysts still has numerous challenges as follows. (1) Deprivation in electrical conductivity of transition metal compounds for OER and HER. (2) More fundamental issue of corrosion in the electrolysis process for basic and acidic media is carbon-based hybrid catalytic products. (3) The inactive existence of transition metal oxides for PEM electrolysis. (4) The lack of relevant knowledge of non-noble metal catalysts and the fundamental chemistry in strong pH media. (5) Fe and Cu are the leading cause of corrosion towards proton ion membranes. (6) There is not enough flexibility in ceramic catalysts for OER and HER to work at higher temperatures. (7) A potential decrease happens because of improper loading of non-noble metal at the anode. (8) Attempts to build bifunctional electrocatalysts for overall OER and HER catalysts are still underway and challenging due to complex synthesis processes. (9) Until now, catalysts have been synthesized with effective improvement compared to noble metals in one aspect, but the challenge is to produce a catalyst with better efficiency than noble metals across the board. (10) The synthesis process plays a significant role in catalyst efficiency by changing their composition and structure.

5.3. Possible Research Directions

Despite the difficulties of discovering the new catalysts required for highly efficient OER and HER processes, there are still many new research possibilities to produce highly efficient catalysts within the field of water electrolysis. Any potential research strategies that might be deserving of exploration are including:

1. The implementation of better, facile, and cost-effective methods for developing highly efficient electrocatalysts for OER and HER based on non-noble metals. New electrocatalysis approaches require either template or template-less systems. However, they also need to be cheap and contain catalysts with diverse properties with highly active surface areas supporting fast reaction kinetics. Besides this, new techniques for the processing of catalysts are required, regulating catalyst morphology.
2. The knowledge of the fundamental processes that generate new OER and HER catalysts. Future studies are expected to establish the catalytic reaction mechanisms of transition metal-based catalysts under various parameters such as pH and temperature conditions. Currently, the pathways of water electrolysis reactions remain unresolved in alkaline conditions, as well as the active center cannot be reliably established. Enhancements in efficiency may be achieved with more excellent knowledge of the compound's comprehensive interpretation mechanism, which would contribute to the improvement in developing effective doping strategies and fabrication methods. Since theoretical simulations and experimental verifications of catalytic processes, such as DFT calculations on atomic levels, should be worked out to better understand the catalyst effect.
3. The studies on the use of low- or non-noble metal-based electrocatalysts in electrolysis are required. Hence, it is required to establish low-/non-noble metal catalysts, which are good enough to work efficiently in neutral to highly acidic environments. The prepared electrocatalysts should have better electrocatalytic efficiency compared to the best noble metal catalysts.
4. The review of low-cost, earth-abundant catalysts for OER and HER in SOECs are required. Because electrode degradation is the biggest issue faced by SOECs, understanding the processes behind the degradation of these catalysts is essential to know in detail for the improvement. This awareness will provide new possibilities for synthesizing an efficient catalytic material for renewable energy production via SOECs.
5. Ultimately, these suggestions for future research will help overcome the existing obstacles in producing successful and broadly available techniques for earth-abundant non-noble metal-based electrocatalysts for water electrolysis.

Funding: This research received no external funding.

Data Availability Statement: No new data were created or analyzed in this study. Data sharing is not applicable to this article.

Acknowledgments: Sami M. Ibn Shamsah extend his appreciation to the University of Hafr Al Batin for providing technical support.

Conflicts of Interest: The author declares no competing financial interests.

References

1. Lewis, N.S.; Nocera, D.G. Powering the planet: Chemical challenges in solar energy utilization. *Proc. Natl. Acad. Sci. USA* **2006**, *103*, 15729–15735. [[CrossRef](#)] [[PubMed](#)]
2. Blankenship, R.E.; Tiede, D.M.; Barber, J.; Brudvig, G.W.; Fleming, G.; Ghirardi, M.; Gunner, M.R.; Junge, W.; Kramer, D.M.; Melis, A.; et al. Comparing photosynthetic and photovoltaic efficiencies and recognizing the potential for improvement. *Science* **2011**, *332*, 805–809. [[CrossRef](#)]
3. Armaroli, N.; Balzani, V. Solar Electricity and Solar Fuels: Status and Perspectives in the Context of the Energy Transition. *Chem. A Eur. J.* **2016**, *22*, 32–57. [[CrossRef](#)] [[PubMed](#)]
4. Styring, S. Artificial photosynthesis for solar fuels. *Faraday Discuss.* **2012**, *155*, 357–376. [[CrossRef](#)] [[PubMed](#)]
5. Le Formal, F.; Bourée, W.S.; Prévot, M.S.; Sivula, K. Challenges towards economic fuel generation from renewable electricity: The need for efficient electrocatalysis. *Chimia* **2015**, *69*, 789–798. [[CrossRef](#)] [[PubMed](#)]
6. Joya, K.S.; Joya, Y.F.; Ocakoglu, K.; van de Krol, R. Water-Splitting Catalysis and Solar Fuel Devices: Artificial Leaves on the Move. *Angew. Chem. Int. Ed.* **2013**, *52*, 10426–10437. [[CrossRef](#)]
7. Tachibana, Y.; Vayssieres, L.; Durrant, J.R. Artificial photosynthesis for solar water-splitting. *Nat. Photonics* **2012**, *6*, 511–518. [[CrossRef](#)]

8. McCrory, C.C.L.; Jung, S.; Ferrer, I.M.; Chatman, S.M.; Peters, J.C.; Jaramillo, T.F. Benchmarking Hydrogen Evolving Reaction and Oxygen Evolving Reaction Electrocatalysts for Solar Water Splitting Devices. *J. Am. Chem. Soc.* **2015**, *137*, 4347–4357. [[CrossRef](#)]
9. Kim, J.; Jun, A.; Gwon, O.; Yoo, S.; Liu, M.; Shin, J.; Lim, T.H.; Kim, G. Hybrid-solid oxide electrolysis cell: A new strategy for efficient hydrogen production. *Nano Energy* **2018**, *44*, 121–126. [[CrossRef](#)]
10. Faber, M.S.; Jin, S. Earth-abundant inorganic electrocatalysts and their nanostructures for energy conversion applications. *Energy Environ. Sci.* **2014**, *7*, 3519–3542. [[CrossRef](#)]
11. Ikhlaiq, A.; Javed, F.; Akram, A.; Qazi, U.Y.; Masood, Z.; Ahmed, T.; Arshad, Z.; Khalid, S.; Qi, F. Treatment of leachate through constructed wetlands using *Typha angustifolia* in combination with catalytic ozonation on Fe-zeolite A. *Int. J. Phytoremediation* **2020**, 1–9. [[CrossRef](#)]
12. Javaid, R.; Tanaka, D.A.P.; Kawanami, H.; Suzuki, T.M. Silica Capillary with Thin Metal (Pd and Pt) Inner Wall: Application to Continuous Decomposition of Hydrogen Peroxide. *Chem. Lett.* **2009**, *38*, 146–147. [[CrossRef](#)]
13. Javaid, R.; Kawanami, H.; Chatterjee, M.; Ishizaka, T.; Suzuki, A.; Suzuki, T.M. Fabrication of microtubular reactors coated with thin catalytic layer (M=Pd, Pd-Cu, Pt, Rh, Au). *Catal. Commun.* **2010**, *11*, 1160–1164. [[CrossRef](#)]
14. Javaid, R.; Kawanami, H.; Chatterjee, M.; Ishizaka, T.; Suzuki, A.; Suzuki, T.M. Sonogashira C-C coupling reaction in water using tubular reactors with catalytic metal inner surface. *Chem. Eng. J.* **2011**, *167*, 431–435. [[CrossRef](#)]
15. Javaid, R.; Kawasaki, S.I.; Suzuki, A.; Suzuki, T.M. Simple and rapid hydrogenation of p-nitrophenol with aqueous formic acid in catalytic flow reactors. *Beilstein J. Org. Chem.* **2013**, *9*, 1156–1163. [[CrossRef](#)]
16. Javaid, R.; Kawasaki, S.; Ookawara, R.; Sato, K.; Nishioka, M.; Suzuki, A.; Suzuki, T.M. Continuous Dehydrogenation of Aqueous Formic Acid under Sub-Critical Conditions by Use of Hollow Tubular Reactor Coated with Thin Palladium Oxide Layer. *J. Chem. Eng. JAPAN* **2013**, *46*, 751–758. [[CrossRef](#)]
17. Javaid, R.; Urata, K.; Furukawa, S.; Komatsu, T. Factors affecting coke formation on H-ZSM-5 in naphtha cracking. *Appl. Catal. A Gen.* **2015**, *491*, 100–105. [[CrossRef](#)]
18. Javaid, R.; Matsumoto, H.; Nanba, T. Influence of Reaction Conditions and Promoting Role of Ammonia Produced at Higher Temperature Conditions in Its Synthesis Process over Cs-Ru/MgO Catalyst. *ChemistrySelect* **2019**, *4*, 2218–2224. [[CrossRef](#)]
19. Dimitriou, P.; Javaid, R. A review of ammonia as a compression ignition engine fuel. *Int. J. Hydrogen Energy* **2020**, *45*, 7098–7118. [[CrossRef](#)]
20. Javaid, R.; Nanba, T. MgFe₂O₄-Supported Ru Catalyst for Ammonia Synthesis: Promotive Effect of Chlorine. *ChemistrySelect* **2020**, *5*, 4312–4315. [[CrossRef](#)]
21. Javaid, R.; Nanba, T. Effect of reaction conditions and surface characteristics of Ru/CeO₂ on catalytic performance for ammonia synthesis as a clean fuel. *Int. J. Hydrogen Energy* **2020**. [[CrossRef](#)]
22. Javaid, R.; Aoki, Y.; Nanba, T. Highly efficient Ru/MgO–Er₂O₃ catalysts for ammonia synthesis. *J. Phys. Chem. Solids* **2020**, *146*, 109570. [[CrossRef](#)]
23. Nanba, T.; Nagata, Y.; Kobayashi, K.; Javaid, R.; Atsumi, R.; Nishi, M.; Mochizuki, T.; Manaka, Y.; Kojima, H.; Tsujimura, T.; et al. Explorative Study of a Ru/CeO₂ Catalyst for NH₃ synthesis from renewable hydrogen and demonstration of NH₃ synthesis under a range of reaction conditions. *J. Japan Pet. Inst.* **2021**, *64*, 1–9. [[CrossRef](#)]
24. Qazi, U.Y.; Kajimoto, S.; Fukumura, H. Effect of Sodium Dodecyl Sulfate on the Formation of Silver Nanoparticles by Biphotonic Reduction of Silver Nitrate in Water. *Chem. Lett.* **2014**, *43*, 1693–1695. [[CrossRef](#)]
25. Javaid, R.; Qazi, U.Y.; Kawasaki, S.-I. Efficient and Continuous Decomposition of Hydrogen Peroxide Using a Silica Capillary Coated with a Thin Palladium or Platinum Layer. *Bull. Chem. Soc. Jpn.* **2015**, *88*, 976–980. [[CrossRef](#)]
26. Qazi, U.Y.; Javaid, R. A Review on Metal Nanostructures: Preparation Methods and Their Potential Applications. *Adv. Nanoparticles* **2016**, *05*, 27–43. [[CrossRef](#)]
27. Javaid, R.; Qazi, U.Y.; Kawasaki, S.I. Highly efficient decomposition of Remazol Brilliant Blue R using tubular reactor coated with thin layer of PdO. *J. Environ. Manag.* **2016**, *180*, 551–556. [[CrossRef](#)]
28. Ullah, N.; Imran, M.; Liang, K.; Yuan, C.Z.; Zeb, A.; Jiang, N.; Qazi, U.Y.; Sahar, S.; Xu, A.W. Highly dispersed ultra-small Pd nanoparticles on gadolinium hydroxide nanorods for efficient hydrogenation reactions. *Nanoscale* **2017**, *9*, 13800–13807. [[CrossRef](#)]
29. Imran, M.; Zhou, X.; Ullah, N.; Liu, Y.-N.; Zeb, A.; Jiang, N.; Qazi, U.Y.; Yuan, C.-Z.; Xu, A.-W. Catalytic Conversion of Biomass into Hydrocarbons over Noble-Metal-Free VO-Substituted Potassium Salt of Phosphotungstic Acid. *ChemistrySelect* **2017**, *2*, 8625–8631. [[CrossRef](#)]
30. Zeb, A.; Sahar, S.; Qazi, U.Y.; Odda, A.H.; Ullah, N.; Liu, Y.N.; Qazi, I.A.; Xu, A.W. Intrinsic peroxidase-like activity and enhanced photo-Fenton reactivity of iron-substituted polyoxometallate nanostructures. *Dalt. Trans.* **2018**, *47*, 7344–7352. [[CrossRef](#)]
31. Yaqub Qazi, U.; Shervani, Z.; Javaid, R. Green Synthesis of Silver Nanoparticles by Pulsed Laser Irradiation: Effect of Hydrophilicity of Dispersing Agents on Size of Particles. *Front. Nanosci. Nanotechnol.* **2018**, *4*. [[CrossRef](#)]
32. Javaid, R.; Qazi, U.Y. Catalytic Oxidation Process for the Degradation of Synthetic Dyes: An Overview. *Int. J. Environ. Res. Public Health* **2019**, *16*, 2066. [[CrossRef](#)] [[PubMed](#)]
33. Rahman, A.; Zulfikar, S.; Haq, A.U.; Alsafari, I.A.; Qazi, U.Y.; Warsi, M.F.; Shahid, M. Cd-Gd-doped nickel spinel ferrite nanoparticles and their nanocomposites with reduced graphene oxide for catalysis and antibacterial activity studies. *Ceram. Int.* **2020**. [[CrossRef](#)]
34. Ahmad Abuilaiwi, F.; Awais, M.; Qazi, U.Y.; Ali, F.; Afzal, A. Al³⁺ doping reduces the electron/hole recombination in photoluminescent copper ferrite (CuFe₂–AlO₄) nanocrystallites. *Boletín la Soc. Española Cerámica y Vidr.* **2020**. [[CrossRef](#)]

35. Tabasum, A.; Alghuthaymi, M.; Qazi, U.Y.; Shahid, I.; Abbas, Q.; Javaid, R.; Nadeem, N.; Zahid, M. UV-Accelerated Photocatalytic Degradation of Pesticide over Magnetite and Cobalt Ferrite Decorated Graphene Oxide Composite. *Plants* **2020**, *10*, 6. [[CrossRef](#)]
36. Roger, I.; Shipman, M.A.; Symes, M.D. Earth-abundant catalysts for electrochemical and photoelectrochemical water splitting. *Nat. Rev. Chem.* **2017**, *1*. [[CrossRef](#)]
37. Nocera, D.G. The artificial leaf. *Acc. Chem. Res.* **2012**, *45*, 767–776. [[CrossRef](#)]
38. Yang, Y.; Tang, Y.; Jiang, H.; Chen, Y.; Wan, P.; Fan, M.; Zhang, R.; Ullah, S.; Pan, L.; Zou, J.J.; et al. 2020 Roadmap on gas-involved photo- and electro- catalysis. *Chin. Chem. Lett.* **2019**, *30*, 2089–2109. [[CrossRef](#)]
39. Dong, H.; Ji, Y.; Ding, L.; Li, Y. Strategies for computational design and discovery of two-dimensional transition-metal-free materials for electrocatalysis applications. *Phys. Chem. Chem. Phys.* **2019**, *21*, 25535–25547. [[CrossRef](#)]
40. Fukuzumi, S.; Yamada, Y.; Suenobu, T.; Ohkubo, K.; Kotani, H. Catalytic mechanisms of hydrogen evolution with homogeneous and heterogeneous catalysts. *Energy Environ. Sci.* **2011**, *4*, 2754–2766. [[CrossRef](#)]
41. Ismail, A.A.; Bahnemann, D.W. Photochemical splitting of water for hydrogen production by photocatalysis: A review. *Solar Energy Mater. Solar Cells* **2014**. [[CrossRef](#)]
42. Parent, A.R.; Sakai, K. Progress in base-metal water oxidation catalysis. *ChemSusChem* **2014**, *7*, 2070–2080. [[CrossRef](#)] [[PubMed](#)]
43. Khan, M.A.; Zhao, H.; Zou, W.; Chen, Z.; Cao, W.; Fang, J.; Xu, J.; Zhang, L.; Zhang, J. Recent Progresses in Electrocatalysts for Water Electrolysis. *Electrochem. Energ. Rev.* **2018**, *1*, 483–530. [[CrossRef](#)]
44. Caldwell, D.L. Production of Chlorine. In *Comprehensive Treatise of Electrochemistry*; Springer: New York, NY, USA, 1981; pp. 105–166.
45. Balat, M. Potential importance of hydrogen as a future solution to environmental and transportation problems. *Int. J. Hydrogen Energy* **2008**, *33*, 4013–4029. [[CrossRef](#)]
46. Blasi, A.; Fiorenza, G.; Freda, C.; Calabrò, V. Steam reforming of biofuels for the production of hydrogen-rich gas. In *Membranes for Clean and Renewable Power Applications*; Elsevier Ltd.: Amsterdam, The Netherlands, 2013; pp. 145–181. ISBN 9780857095459.
47. Serban, M.; Lewis, M.A.; Marshall, C.L.; Doctor, R.D. Hydrogen production by direct contact pyrolysis of natural gas. *Energy Fuels* **2003**, *17*, 705–713. [[CrossRef](#)]
48. Schlapbach, L.; Züttel, A. Hydrogen-storage materials for mobile applications. In *Materials for Sustainable Energy: A Collection of Peer-Reviewed Research and Review Articles from Nature Publishing Group*; World Scientific Publishing Co.: London, UK, 2010; pp. 265–270. ISBN 9789814317665.
49. Carmo, M.; Fritz, D.L.; Mergel, J.; Stolten, D. A comprehensive review on PEM water electrolysis. *Int. J. Hydrog. Energy* **2013**, *38*, 4901–4934. [[CrossRef](#)]
50. Choi, P.; Bessarabov, D.G.; Datta, R. A simple model for solid polymer electrolyte (SPE) water electrolysis. *Solid State Ion.* **2004**, *175*, 535–539. [[CrossRef](#)]
51. Ursúa, A.; Gandía, L.M.; Sanchis, P. Hydrogen production from water electrolysis: Current status and future trends. *Proc. IEEE* **2012**, *100*, 410–426. [[CrossRef](#)]
52. Holladay, J.D.; Hu, J.; King, D.L.; Wang, Y. An overview of hydrogen production technologies. *Catal. Today* **2009**, *139*, 244–260. [[CrossRef](#)]
53. Tahir, M.; Pan, L.; Idrees, F.; Zhang, X.; Wang, L.; Zou, J.J.; Wang, Z.L. Electrocatalytic oxygen evolution reaction for energy conversion and storage: A comprehensive review. *Nano Energy* **2017**, *37*, 136–157. [[CrossRef](#)]
54. Yue, Y.; Zhu, Y.; Li, F.; Xue, T. Fabrication and Characterization of Controlled-Morphology Self-Supported Fe/Co Layered Double Hydroxides as Catalysts for the Oxygen Evolution Reaction. *Catal. Lett.* **2020**, *151*, 507–516. [[CrossRef](#)]
55. Liu, H.; Xi, C.; Xin, J.; Zhang, G.; Zhang, S.; Zhang, Z.; Huang, Q.; Li, J.; Liu, H.; Kang, J. Free-standing nanoporous NiMnFeMo alloy: An efficient non-precious metal electrocatalyst for water splitting. *Chem. Eng. J.* **2021**, *404*, 126530. [[CrossRef](#)]
56. Li, R.-Q.; Liu, Q.; Zhou, Y.; Lu, M.; Hou, J.; Qu, K.; Zhu, Y.; Fontaine, O. 3D self-supported porous vanadium-doped nickel nitride nanosheet arrays as efficient bifunctional electrocatalysts for urea electrolysis. *J. Mater. Chem. A* **2021**. [[CrossRef](#)]
57. Yu, F.; Yu, L.; Mishra, I.K.; Yu, Y.; Ren, Z.F.; Zhou, H.Q. Recent developments in earth-abundant and non-noble electrocatalysts for water electrolysis. *Mater. Today Phys.* **2018**, *7*, 121–138. [[CrossRef](#)]
58. Anantharaj, S.; Noda, S.; Jothi, V.R.; Yi, S.; Driess, M.; Menezes, P.W. Strategies and Perspectives to Catch the Missing Pieces in Energy-Efficient Hydrogen Evolution Reaction in Alkaline Media. *Angew. Chemie Int. Ed.* **2021**. [[CrossRef](#)]
59. Panda, C.; Menezes, P.W.; Driess, M. Nano-Sized Inorganic Energy-Materials by the Low-Temperature Molecular Precursor Approach. *Angew. Chemie Int. Ed.* **2018**, *57*, 11130–11139. [[CrossRef](#)]
60. Cheng, X.; Li, Y.; Zheng, L.; Yan, Y.; Zhang, Y.; Chen, G.; Sun, S.; Zhang, J. Highly active, stable oxidized platinum clusters as electrocatalysts for the hydrogen evolution reaction. *Energy Environ. Sci.* **2017**, *10*, 2450–2458. [[CrossRef](#)]
61. Lima, D.W.; Fiegenbaum, F.; Trombetta, F.; de Souza, M.O.; Martini, E.M.A. PtNi and PtMo nanoparticles as efficient catalysts using TEA-PS.BF4 ionic liquid as electrolyte towards HER. *Int. J. Hydrog. Energy* **2017**, *42*, 5676–5683. [[CrossRef](#)]
62. Ma, R.; Zhou, Y.; Wang, F.; Yan, K.; Liu, Q.; Wang, J. Efficient electrocatalysis of hydrogen evolution by ultralow-Pt-loading bamboo-like nitrogen-doped carbon nanotubes. *Mater. Today Energy* **2017**, *6*, 173–180. [[CrossRef](#)]
63. Luo, B.; Yan, X.; Chen, J.; Xu, S.; Xue, Q. PtFe nanotubes/graphene hybrid: Facile synthesis and its electrochemical properties. *Int. J. Hydrog. Energy* **2013**, *38*, 13011–13016. [[CrossRef](#)]

64. Gabler, A.; Müller, C.I.; Rauscher, T.; Gimpel, T.; Hahn, R.; Köhring, M.; Kieback, B.; Röntzsch, L.; Schade, W. Ultrashort-pulse laser structured titanium surfaces with sputter-coated platinum catalyst as hydrogen evolution electrodes for alkaline water electrolysis. *Int. J. Hydrog. Energy* **2018**, *43*, 7216–7226. [[CrossRef](#)]
65. Zheng, J. Binary platinum alloy electrodes for hydrogen and oxygen evolutions by seawater splitting. *Appl. Surf. Sci.* **2017**, *413*, 72–82. [[CrossRef](#)]
66. Ren, F.; Zhou, W.; Du, Y.; Yang, P.; Wang, C.; Xu, J. High efficient electrocatalytic oxidation of formic acid at Pt dispersed on porous poly(o-methoxyaniline). *Int. J. Hydrog. Energy* **2011**, *36*, 6414–6421. [[CrossRef](#)]
67. Fang, M.; Gao, W.; Dong, G.; Xia, Z.; Yip, S.; Qin, Y.; Qu, Y.; Ho, J.C. Hierarchical NiMo-based 3D electrocatalysts for highly-efficient hydrogen evolution in alkaline conditions. *Nano Energy* **2016**, *27*, 247–254. [[CrossRef](#)]
68. Sun, T.; Xu, L.; Yan, Y.; Zakhidov, A.A.; Baughman, R.H.; Chen, J. Ordered Mesoporous Nickel Sphere Arrays for Highly Efficient Electrocatalytic Water Oxidation. *ACS Catal.* **2016**, *6*, 1446–1450. [[CrossRef](#)]
69. Zhang, J.; Baró, M.D.; Pellicer, E.; Sort, J. Electrodeposition of magnetic, superhydrophobic, non-stick, two-phase Cu-Ni foam films and their enhanced performance for hydrogen evolution reaction in alkaline water media. *Nanoscale* **2014**, *6*, 12490–12499. [[CrossRef](#)] [[PubMed](#)]
70. Yin, Z.; Chen, F. A facile electrochemical fabrication of hierarchically structured nickel-copper composite electrodes on nickel foam for hydrogen evolution reaction. *J. Power Sources* **2014**, *265*, 273–281. [[CrossRef](#)]
71. Hong, S.H.; Ahn, S.H.; Choi, J.; Kim, J.Y.; Kim, H.Y.; Kim, H.J.; Jang, J.H.; Kim, H.; Kim, S.K. High-activity electrodeposited NiW catalysts for hydrogen evolution in alkaline water electrolysis. *Appl. Surf. Sci.* **2015**, *349*, 629–635. [[CrossRef](#)]
72. He, X.D.; Xu, F.; Li, F.; Liu, L.; Wang, Y.; Deng, N.; Zhu, Y.W.; He, J.B. Composition-performance relationship of Ni_xCu_y nanoalloys as hydrogen evolution electrocatalyst. *J. Electroanal. Chem.* **2017**, *799*, 235–241. [[CrossRef](#)]
73. Zhu, Y.; Zhang, X.; Song, J.; Wang, W.; Yue, F.; Ma, Q. Microstructure and hydrogen evolution catalytic properties of Ni-Sn alloys prepared by electrodeposition method. *Appl. Catal. A Gen.* **2015**, *500*, 51–57. [[CrossRef](#)]
74. Wang, X.; Su, R.; Aslan, H.; Kibsgaard, J.; Wendt, S.; Meng, L.; Dong, M.; Huang, Y.; Besenbacher, F. Tweaking the composition of NiMoZn alloy electrocatalyst for enhanced hydrogen evolution reaction performance. *Nano Energy* **2015**, *12*, 9–18. [[CrossRef](#)]
75. Yang, Q.; Lv, C.; Huang, Z.; Zhang, C. Amorphous film of ternary Ni-Co-P alloy on Ni foam for efficient hydrogen evolution by electroless deposition. *Int. J. Hydrog. Energy* **2018**, *43*, 7872–7880. [[CrossRef](#)]
76. Yüce, A.O.; Döner, A.; Kardaş, G. NiMn composite electrodes as cathode material for hydrogen evolution reaction in alkaline solution. *Int. J. Hydrog. Energy* **2013**, *38*, 4466–4473. [[CrossRef](#)]
77. Rauscher, T.; Müller, C.I.; Schmidt, A.; Kieback, B.; Röntzsch, L. Ni-Mo-B alloys as cathode material for alkaline water electrolysis. *Int. J. Hydrog. Energy* **2016**, *41*, 2165–2176. [[CrossRef](#)]
78. Schalenbach, M.; Speck, F.D.; Ledendecker, M.; Kasian, O.; Goehl, D.; Mingers, A.M.; Breitbach, B.; Springer, H.; Cherevko, S.; Mayrhofer, K.J.J. Nickel-molybdenum alloy catalysts for the hydrogen evolution reaction: Activity and stability revised. *Electrochim. Acta* **2018**, *259*, 1154–1161. [[CrossRef](#)]
79. Guo, H.; Youliwasi, N.; Zhao, L.; Chai, Y.; Liu, C. Carbon-encapsulated nickel-cobalt alloys nanoparticles fabricated via new post-treatment strategy for hydrogen evolution in alkaline media. *Appl. Surf. Sci.* **2018**, *435*, 237–246. [[CrossRef](#)]
80. Trasatti, S. Work function, electronegativity, and electrochemical behaviour of metals. III. Electrolytic hydrogen evolution in acid solutions. *J. Electroanal. Chem.* **1972**, *39*, 163–184. [[CrossRef](#)]
81. Sheng, W.; Myint, M.; Chen, J.G.; Yan, Y. Correlating the hydrogen evolution reaction activity in alkaline electrolytes with the hydrogen binding energy on monometallic surfaces. *Energy Environ. Sci.* **2013**, *6*, 1509–1512. [[CrossRef](#)]
82. Nørskov, J.K.; Bligaard, T.; Logadottir, A.; Kitchin, J.R.; Chen, J.G.; Pandelov, S.; Stimming, U. Trends in the Exchange Current for Hydrogen Evolution. *J. Electrochem. Soc.* **2005**, *152*, J23. [[CrossRef](#)]
83. Hinnemann, B.; Moses, P.G.; Bonde, J.; Jørgensen, K.P.; Nielsen, J.H.; Horch, S.; Chorkendorff, I.; Nørskov, J.K. Biomimetic hydrogen evolution: MoS₂ nanoparticles as catalyst for hydrogen evolution. *J. Am. Chem. Soc.* **2005**, *127*, 5308–5309. [[CrossRef](#)]
84. Jaegermann, W.; Tributsch, H. Interfacial properties of semiconducting transition metal chalcogenides. *Prog. Surf. Sci.* **1988**, *29*, 1–167. [[CrossRef](#)]
85. Wiltmans, R.; Vink, M.K.; Schoemaker, H.E.; van Delft, F.L.; Blaauw, R.H.; Rutjes, F.P. libro blanco para la minimización de residuos y emisiones. *Synthesis* **2004**, *2004*, 641–662.
86. Jaramillo, T.F.; Jørgensen, K.P.; Bonde, J.; Nielsen, J.H.; Horch, S.; Chorkendorff, I. Identification of active edge sites for electrochemical H₂ evolution from MoS₂ nanocatalysts. *Science* **2007**, *317*, 100–102. [[CrossRef](#)] [[PubMed](#)]
87. Zhou, H.; Wang, Y.; He, R.; Yu, F.; Sun, J.; Wang, F.; Lan, Y.; Ren, Z.; Chen, S. One-step synthesis of self-supported porous NiSe₂/Ni hybrid foam: An efficient 3D electrode for hydrogen evolution reaction. *Nano Energy* **2016**, *20*, 29–36. [[CrossRef](#)]
88. Kiran, V.; Mukherjee, D.; Jenjeti, R.N.; Sampath, S. Active guests in the MoS₂/MoSe₂ host lattice: Efficient hydrogen evolution using few-layer alloys of MoS₂(1-x)Se_{2x}. *Nanoscale* **2014**, *6*, 12856–12863. [[CrossRef](#)]
89. Voiry, D.; Yamaguchi, H.; Li, J.; Silva, R.; Alves, D.C.B.; Fujita, T.; Chen, M.; Asefa, T.; Shenoy, V.B.; Eda, G.; et al. Enhanced catalytic activity in strained chemically exfoliated WS₂ nanosheets for hydrogen evolution. *Nat. Mater.* **2013**, *12*, 850–855. [[CrossRef](#)] [[PubMed](#)]
90. Tran, P.D.; Chiam, S.Y.; Boix, P.P.; Ren, Y.; Pramana, S.S.; Fize, J.; Artero, V.; Barber, J. Novel cobalt/nickel-tungsten-sulfide catalysts for electrocatalytic hydrogen generation from water. *Energy Environ. Sci.* **2013**, *6*, 2452–2459. [[CrossRef](#)]

91. Sun, Y.; Liu, C.; Grauer, D.C.; Yano, J.; Long, J.R.; Yang, P.; Chang, C.J. Electrodeposited cobalt-sulfide catalyst for electrochemical and photoelectrochemical hydrogen generation from water. *J. Am. Chem. Soc.* **2013**, *135*, 17699–17702. [CrossRef] [PubMed]
92. Faber, M.S.; Dzedzic, R.; Lukowski, M.A.; Kaiser, N.S.; Ding, Q.; Jin, S. High-performance electrocatalysis using metallic cobalt pyrite (CoS₂) micro- and nanostructures. *J. Am. Chem. Soc.* **2014**, *136*, 10053–10061. [CrossRef] [PubMed]
93. Li, H.; Tsai, C.; Koh, A.L.; Cai, L.; Contryman, A.W.; Fragapane, A.H.; Zhao, J.; Han, H.S.; Manoharan, H.C.; Abild-Pedersen, F.; et al. Activating and optimizing MoS₂ basal planes for hydrogen evolution through the formation of strained sulphur vacancies. *Nat. Mater.* **2016**, *15*, 48–53. [CrossRef]
94. Li, Y.; Wang, H.; Xie, L.; Liang, Y.; Hong, G.; Dai, H. MoS₂ nanoparticles grown on graphene: An advanced catalyst for the hydrogen evolution reaction. *J. Am. Chem. Soc.* **2011**, *133*, 7296–7299. [CrossRef]
95. Merki, D.; Fierro, S.; Vrabel, H.; Hu, X. Amorphous molybdenum sulfide films as catalysts for electrochemical hydrogen production in water. *Chem. Sci.* **2011**, *2*, 1262–1267. [CrossRef]
96. Li, X.; Zhao, L.; Yu, J.; Liu, X.; Zhang, X.; Liu, H.; Zhou, W. Water Splitting: From Electrode to Green Energy System. *Nano Micro Lett.* **2020**, *12*, 1–29. [CrossRef]
97. Mohammed-Ibrahim, J.; Xiaoming, S. Recent progress on earth abundant electrocatalysts for hydrogen evolution reaction (HER) in alkaline medium to achieve efficient water splitting—A review. *J. Energy Chem.* **2019**, *34*, 111–160. [CrossRef]
98. Popczun, E.J.; McKone, J.R.; Read, C.G.; Biacchi, A.J.; Wiltrout, A.M.; Lewis, N.S.; Schaak, R.E. Nanostructured Nickel Phosphide as an Electrocatalyst for the Hydrogen Evolution Reaction. *J. Am. Chem. Soc.* **2013**, *135*, 9267–9270. Available online: <https://pubs.acs.org/doi/10.1021/ja403440e> (accessed on 21 February 2021). [CrossRef] [PubMed]
99. Popczun, E.J.; Read, C.G.; Roske, C.W.; Lewis, N.S.; Schaak, R.E. Highly active electrocatalysis of the hydrogen evolution reaction by cobalt phosphide nanoparticles. *Angew. Chem. Int. Ed.* **2014**, *53*, 5427–5430. [CrossRef] [PubMed]
100. Jiang, P.; Liu, Q.; Liang, Y.; Tian, J.; Asiri, A.M.; Sun, X. A Cost-Effective 3D Hydrogen Evolution Cathode with High Catalytic Activity: FeP Nanowire Array as the Active Phase. *Angew. Chem. Int. Ed.* **2014**, *53*, 12855–12859. [CrossRef]
101. Kibsgaard, J.; Jaramillo, T.F. Molybdenum Phosphosulfide: An Active, Acid-Stable, Earth-Abundant Catalyst for the Hydrogen Evolution Reaction. *Angew. Chem. Int. Ed.* **2014**, *53*, 14433–14437. [CrossRef]
102. Chen, Z.; Wei, W.; Ni, B.J. Cost-effective catalysts for renewable hydrogen production via electrochemical water splitting: Recent advances. *Curr. Opin. Green Sustain. Chem.* **2021**, *27*, 100398. [CrossRef]
103. Boppella, R.; Tan, J.; Yun, J.; Manorama, S.V.; Moon, J. Anion-mediated transition metal electrocatalysts for efficient water electrolysis: Recent advances and future perspectives. *Coord. Chem. Rev.* **2021**, *427*, 213552. [CrossRef]
104. Jin, D.; Johnson, L.R.; Raman, A.S.; Ming, X.; Gao, Y.; Du, F.; Wei, Y.; Chen, G.; Vojvodic, A.; Gogotsi, Y.; et al. Computational Screening of 2D Ordered Double Transition-Metal Carbides (MXenes) as Electrocatalysts for Hydrogen Evolution Reaction. *J. Phys. Chem. C* **2020**, *124*, 10584–10592. [CrossRef]
105. Hu, W.; Shi, Q.; Chen, Z.; Yin, H.; Zhong, H.; Wang, P. Co₂N/Co₂Mo₃O₈ Heterostructure as a Highly Active Electrocatalyst for an Alkaline Hydrogen Evolution Reaction. *Acs Appl. Mater. Interfaces* **2021**, acsami.0c20271. [CrossRef]
106. Cao, B.; Veith, G.M.; Neufeind, J.C.; Adzic, R.R.; Khalifah, P.G. Mixed close-packed cobalt molybdenum nitrides as non-noble metal electrocatalysts for the hydrogen evolution reaction. *J. Am. Chem. Soc.* **2013**, *135*, 19186–19192. [CrossRef]
107. Chen, W.-F.; Sasaki, K.; Ma, C.; Frenkel, A.I.; Marinkovic, N.; Muckerman, J.T.; Zhu, Y.; Adzic, R.R. Hydrogen-Evolution Catalysts Based on Non-Noble Metal Nickel-Molybdenum Nitride Nanosheets. *Angew. Chem. Int. Ed.* **2012**, *51*, 6131–6135. [CrossRef]
108. Liang, H.W.; Brüller, S.; Dong, R.; Zhang, J.; Feng, X.; Müllen, K. Molecular metal-N_x centres in porous carbon for electrocatalytic hydrogen evolution. *Nat. Commun.* **2015**, *6*, 1–8. [CrossRef]
109. Jiao, M.; Chen, Z.; Zhang, X.; Mou, K.; Liu, L. Multicomponent N doped graphene coating Co@Zn heterostructures electrocatalysts as high efficiency HER electrocatalyst in alkaline electrolyte. *Int. J. Hydrog. Energy* **2020**, *45*, 16326–16336. [CrossRef]
110. Ge, R.; Huo, J.; Liao, T.; Liu, Y.; Zhu, M.; Li, Y.; Zhang, J.; Li, W. Hierarchical molybdenum phosphide coupled with carbon as a whole pH-range electrocatalyst for hydrogen evolution reaction. *Appl. Catal. B Environ.* **2020**, *260*, 118196. [CrossRef]
111. Das, D.; Nanda, K.K. One-step, integrated fabrication of Co₂P nanoparticles encapsulated N, P dual-doped CNTs for highly advanced total water splitting. *Nano Energy* **2016**, *30*, 303–311. [CrossRef]
112. Lei, C.; Wang, Y.; Hou, Y.; Liu, P.; Yang, J.; Zhang, T.; Zhuang, X.; Chen, M.; Yang, B.; Lei, L.; et al. Efficient alkaline hydrogen evolution on atomically dispersed Ni-N_x Species anchored porous carbon with embedded Ni nanoparticles by accelerating water dissociation kinetics. *Energy Environ. Sci.* **2019**, *12*, 149–156. [CrossRef]
113. Liu, Q.; Tian, J.; Cui, W.; Jiang, P.; Cheng, N.; Asiri, A.M.; Sun, X. Carbon Nanotubes Decorated with CoP Nanocrystals: A Highly Active Non-Noble-Metal Nanohybrid Electrocatalyst for Hydrogen Evolution. *Angew. Chem. Int. Ed.* **2014**, *53*, 6710–6714. [CrossRef] [PubMed]
114. Li, D.J.; Maiti, U.N.; Lim, J.; Choi, D.S.; Lee, W.J.; Oh, Y.; Lee, G.Y.; Kim, S.O. Molybdenum sulfide/N-doped CNT forest hybrid catalysts for high-performance hydrogen evolution reaction. *Nano Lett.* **2014**, *14*, 1228–1233. [CrossRef] [PubMed]
115. Tabassum, H.; Guo, W.; Meng, W.; Mahmood, A.; Zhao, R.; Wang, Q.; Zou, R. Hydrogen Evolution: Metal-Organic Frameworks Derived Cobalt Phosphide Architecture Encapsulated into B/N Co-Doped Graphene Nanotubes for All pH Value Electrochemical Hydrogen Evolution (Adv. Energy Mater. 9/2017). *Adv. Energy Mater.* **2017**, *7*. [CrossRef]
116. Zheng, J.; Chen, X.; Zhong, X.; Li, S.; Liu, T.; Zhuang, G.; Li, X.; Deng, S.; Mei, D.; Wang, J.-G. Hierarchical Porous NC@CuCo Nitride Nanosheet Networks: Highly Efficient Bifunctional Electrocatalyst for Overall Water Splitting and Selective Electrooxidation of Benzyl Alcohol. *Adv. Funct. Mater.* **2017**, *27*, 1704169. [CrossRef]

117. Xiong, W.; Guo, Q.; Guo, Z.; Li, H.; Zhao, R.; Chen, Q.; Liu, Z.; Wang, X. Atomic layer deposition of nickel carbide for supercapacitors and electrocatalytic hydrogen evolution. *J. Mater. Chem. A* **2018**, *6*, 4297–4304. [[CrossRef](#)]
118. Lin, H.; Zhang, W.; Shi, Z.; Che, M.; Yu, X.; Tang, Y.; Gao, Q. Electrospinning Hetero-Nanofibers of Fe₃C-Mo₂C/Nitrogen-Doped-Carbon as Efficient Electrocatalysts for Hydrogen Evolution. *ChemSusChem* **2017**, *10*, 2597–2604. [[CrossRef](#)] [[PubMed](#)]
119. Zhang, B.; Hou, J.; Wu, Y.; Cao, S.; Li, Z.; Nie, X.; Gao, Z.; Sun, L. Tailoring Active Sites in Mesoporous Defect-Rich NC/V o-WON Heterostructure Array for Superior Electrocatalytic Hydrogen Evolution. *Adv. Energy Mater.* **2019**, *9*. [[CrossRef](#)]
120. Wu, C.; Liu, D.; Li, H.; Li, J. Molybdenum Carbide-Decorated Metallic Cobalt@Nitrogen-Doped Carbon Polyhedrons for Enhanced Electrocatalytic Hydrogen Evolution. *Small* **2018**, *14*, 1704227. [[CrossRef](#)]
121. Zhou, M.; Weng, Q.; Popov, Z.I.; Yang, Y.; Antipina, L.Y.; Sorokin, P.B.; Wang, X.; Bando, Y.; Golberg, D. Construction of Polarized Carbon-Nickel Catalytic Surfaces for Potent, Durable, and Economic Hydrogen Evolution Reactions. *ACS Nano* **2018**, *12*, 4148–4155. [[CrossRef](#)]
122. Qazi, U.Y.; Javaid, R.; Tahir, N.; Jamil, A.; Afzal, A. Design of advanced self-supported electrode by surface modification of copper foam with transition metals for efficient hydrogen evolution reaction. *Int. J. Hydrog. Energy* **2020**, *45*, 33396–33406. [[CrossRef](#)]
123. Jing, S.; Zhang, L.; Luo, L.; Lu, J.; Yin, S.; Shen, P.K.; Tsiakaras, P. N-Doped Porous Molybdenum Carbide Nanobelts as Efficient Catalysts for Hydrogen Evolution Reaction. *Appl. Catal. B Environ.* **2018**, *224*, 533–540. [[CrossRef](#)]
124. Pu, Z.; Wei, S.; Chen, Z.; Mu, S. Flexible molybdenum phosphide nanosheet array electrodes for hydrogen evolution reaction in a wide pH range. *Appl. Catal. B Environ.* **2016**, *196*, 193–198. [[CrossRef](#)]
125. Qian, X.; Ding, J.; Zhang, J.; Zhang, Y.; Wang, Y.; Kan, E.; Wang, X.; Zhu, J. Ultrathin molybdenum disulfide/carbon nitride nanosheets with abundant active sites for enhanced hydrogen evolution. *Nanoscale* **2018**, *10*, 1766–1773. [[CrossRef](#)] [[PubMed](#)]
126. Ansovini, D.; Jun Lee, C.J.; Chua, C.S.; Ong, L.T.; Tan, H.R.; Webb, W.R.; Raja, R.; Lim, Y.F. A highly active hydrogen evolution electrocatalyst based on a cobalt-nickel sulfide composite electrode. *J. Mater. Chem. A* **2016**, *4*, 9744–9749. [[CrossRef](#)]
127. Lin, Y.; Pan, Y.; Zhang, J. CoP nanorods decorated biomass derived N, P co-doped carbon flakes as an efficient hybrid catalyst for electrochemical hydrogen evolution. *Electrochim. Acta* **2017**, *232*, 561–569. [[CrossRef](#)]
128. Tao, K.; Gong, Y.; Lin, J. Low-temperature synthesis of NiS/MoS₂/C nanowires/nanoflakes as electrocatalyst for hydrogen evolution reaction in alkaline medium via calcining/sulfurizing metal-organic frameworks. *Electrochim. Acta* **2018**, *274*, 74–83. [[CrossRef](#)]
129. Mugheri, A.Q.; Ali, S.; Narejo, G.S.; Otho, A.A.; Lal, R.; Abro, M.A.; Memon, S.H.; Abbasi, F. Electrospun fibrous active bimetallic electrocatalyst for hydrogen evolution. *Int. J. Hydrog. Energy* **2020**, *45*, 21502–21511. [[CrossRef](#)]
130. Zhang, J.; Wang, T.; Liu, P.; Liu, S.; Dong, R.; Zhuang, X.; Chen, M.; Feng, X. Engineering water dissociation sites in MoS₂ nanosheets for accelerated electrocatalytic hydrogen production. *Energy Environ. Sci.* **2016**, *9*, 2789–2793. [[CrossRef](#)]
131. Zhang, B.; Liu, J.; Wang, J.; Ruan, Y.; Ji, X.; Xu, K.; Chen, C.; Wan, H.; Miao, L.; Jiang, J. Interface engineering: The Ni(OH)₂/MoS₂ heterostructure for highly efficient alkaline hydrogen evolution. *Nano Energy* **2017**, *37*, 74–80. [[CrossRef](#)]
132. Wang, C.; Tian, B.; Wu, M.; Wang, J. Revelation of the Excellent Intrinsic Activity of MoS₂|NiS|MoO₃ Nanowires for Hydrogen Evolution Reaction in Alkaline Medium. *ACS Appl. Mater. Interfaces* **2017**, *9*, 7084–7090. [[CrossRef](#)]
133. Meiron, O.E.; Kuraganti, V.; Hod, I.; Bar-Ziv, R.; Bar-Sadan, M. Improved catalytic activity of Mo1-: XW_xSe₂ alloy nanoflowers promotes efficient hydrogen evolution reaction in both acidic and alkaline aqueous solutions. *Nanoscale* **2017**, *9*, 13998–14005. [[CrossRef](#)]
134. Zhao, G.; Li, P.; Rui, K.; Chen, Y.; Dou, S.X.; Sun, W. CoSe₂/MoSe₂ Heterostructures with Enriched Water Adsorption/Dissociation Sites towards Enhanced Alkaline Hydrogen Evolution Reaction. *Chem. A Eur. J.* **2018**, *24*, 11158–11165. [[CrossRef](#)]
135. Zhao, G.; Lin, Y.; Rui, K.; Zhou, Q.; Chen, Y.; Dou, S.X.; Sun, W. Epitaxial growth of Ni(OH)₂ nanoclusters on MoS₂ nanosheets for enhanced alkaline hydrogen evolution reaction. *Nanoscale* **2018**, *10*, 19074–19081. [[CrossRef](#)]
136. Li, L.; Sun, C.; Shang, B.; Li, Q.; Lei, J.; Li, N.; Pan, F. Tailoring the facets of Ni₃S₂ as a bifunctional electrocatalyst for high-performance overall water-splitting. *J. Mater. Chem. A* **2019**, *7*, 18003–18011. [[CrossRef](#)]
137. Lin, J.; Yan, Y.; Li, C.; Si, X.; Wang, H.; Qi, J.; Cao, J.; Zhong, Z.; Fei, W.; Feng, J. Bifunctional Electrocatalysts Based on Mo-Doped NiCoP Nanosheet Arrays for Overall Water Splitting. *Nano Micro Lett.* **2019**, *11*, 1–11. [[CrossRef](#)]
138. Yuan, Z.; Li, J.; Yang, M.; Fang, Z.; Jian, J.; Yu, D.; Chen, X.; Dai, L. Ultrathin Black Phosphorus-on-Nitrogen Doped Graphene for Efficient Overall Water Splitting: Dual Modulation Roles of Directional Interfacial Charge Transfer. *J. Am. Chem. Soc.* **2019**, *141*, 4972–4979. [[CrossRef](#)] [[PubMed](#)]
139. Fan, L.; Liu, P.F.; Yan, X.; Gu, L.; Yang, Z.Z.; Yang, H.G.; Qiu, S.; Yao, X. Atomically isolated nickel species anchored on graphitized carbon for efficient hydrogen evolution electrocatalysis. *Nat. Commun.* **2016**, *7*, 1–7. [[CrossRef](#)] [[PubMed](#)]
140. Lu, Q.; Hutchings, G.S.; Yu, W.; Zhou, Y.; Forest, R.V.; Tao, R.; Rosen, J.; Yonemoto, B.T.; Cao, Z.; Zheng, H.; et al. Highly porous non-precious bimetallic electrocatalysts for efficient hydrogen evolution. *Nat. Commun.* **2015**, *6*, 1–8. [[CrossRef](#)] [[PubMed](#)]
141. Merrill, M.D.; Dougherty, R.C. Metal oxide catalysts for the evolution of O₂ from H₂O. *J. Phys. Chem. C* **2008**, *112*, 3655–3666. [[CrossRef](#)]
142. Li, X.; Walsh, F.C.; Pletcher, D. Nickel Based Electrocatalysts for Oxygen Evolution in High Current Density, Alkaline Water Electrolysers. *Phys. Chem. Chem. Phys.* **2011**, *13*, 1162–1167. [[CrossRef](#)]
143. Corrigan, D.A. The Catalysis of the Oxygen Evolution Reaction by Iron Impurities in Thin Film Nickel Oxide Electrodes. *J. Electrochem. Soc.* **1987**, *134*, 377–384. [[CrossRef](#)]

144. Louie, M.W.; Bell, A.T. An investigation of thin-film Ni-Fe oxide catalysts for the electrochemical evolution of oxygen. *J. Am. Chem. Soc.* **2013**, *135*, 12329–12337. [[CrossRef](#)] [[PubMed](#)]
145. Li, H.; Wang, J.; Qi, R.; Hu, Y.; Zhang, J.; Zhao, H.; Zhang, J.; Zhao, Y. Enhanced Fe 3d delocalization and moderate spin polarization in Fe[*s*nd]Ni atomic pairs for bifunctional ORR and OER electrocatalysis. *Appl. Catal. B Environ.* **2021**, *285*, 119778. [[CrossRef](#)]
146. Ying, M.; Tang, R.; Yang, W.; Liang, W.; Yang, G.; Pan, H.; Liao, X.; Huang, J. Tailoring Electronegativity of Bimetallic Ni/Fe Metal-Organic Framework Nanosheets for Electrocatalytic Water Oxidation. *ACS Appl. Nano Mater.* **2021**. [[CrossRef](#)]
147. Lambert, T.N.; Vigil, J.A.; White, S.E.; Davis, D.J.; Limmer, S.J.; Burton, P.D.; Coker, E.N.; Beechem, T.E.; Brumbach, M.T. Electrodeposited $\text{Ni}_x\text{Co}_{3-x}\text{O}_4$ nanostructured films as bifunctional oxygen electrocatalysts. *Chem. Commun.* **2015**, *51*, 9511–9514. [[CrossRef](#)]
148. Tian, J.; Cheng, N.; Liu, Q.; Sun, X.; He, Y.; Asiri, A.M. Self-supported NiMo hollow nanorod array: An efficient 3D bifunctional catalytic electrode for overall water splitting. *J. Mater. Chem. A* **2015**, *3*, 20056–20059. [[CrossRef](#)]
149. Trotochaud, L.; Young, S.L.; Ranney, J.K.; Boettcher, S.W. Nickel-Iron oxyhydroxide oxygen-evolution electrocatalysts: The role of intentional and incidental iron incorporation. *J. Am. Chem. Soc.* **2014**, *136*, 6744–6753. [[CrossRef](#)]
150. Smith, A.M.; Trotochaud, L.; Burke, M.S.; Boettcher, S.W. Contributions to activity enhancement via Fe incorporation in Ni-(oxy)hydroxide/borate catalysts for near-neutral pH oxygen evolution. *Chem. Commun.* **2015**, *51*, 5261–5263. [[CrossRef](#)]
151. Burke, M.S.; Kast, M.G.; Trotochaud, L.; Smith, A.M.; Boettcher, S.W. Cobalt-Iron (Oxy)hydroxide Oxygen Evolution Electrocatalysts: The Role of Structure and Composition on Activity, Stability, and Mechanism. *J. Am. Chem. Soc.* **2015**, *137*, 3638–3648. [[CrossRef](#)]
152. Roger, I.; Symes, M.D. Efficient Electrocatalytic Water Oxidation at Neutral and High pH by Adventitious Nickel at Nanomolar Concentrations. *J. Am. Chem. Soc.* **2015**, *137*, 13980–13988. [[CrossRef](#)]
153. Zou, H.H.; Yuan, C.Z.; Zou, H.Y.; Cheang, T.Y.; Zhao, S.J.; Qazi, U.Y.; Zhong, S.L.; Wang, L.; Xu, A.W. Bimetallic phosphide hollow nanocubes derived from a prussian-blue-analog used as high-performance catalysts for the oxygen evolution reaction. *Catal. Sci. Technol.* **2017**, *7*, 1549–1555. [[CrossRef](#)]
154. Qazi, U.Y.; Yuan, C.Z.; Ullah, N.; Jiang, Y.F.; Imran, M.; Zeb, A.; Zhao, S.J.; Javaid, R.; Xu, A.W. One-Step Growth of Iron-Nickel Bimetallic Nanoparticles on FeNi Alloy Foils: Highly Efficient Advanced Electrodes for the Oxygen Evolution Reaction. *ACS Appl. Mater. Interfaces* **2017**, *9*, 28627–28634. [[CrossRef](#)] [[PubMed](#)]
155. Bao, W.; Xiao, L.; Zhang, J.; Jiang, P.; Zou, X.; Yang, C.; Hao, X.; Ai, T. Electronic and structural engineering of $\text{NiCo}_2\text{O}_4/\text{Ti}$ electrocatalysts for efficient oxygen evolution reaction. *Int. J. Hydrog. Energy* **2021**. [[CrossRef](#)]
156. Feng, H.; Sun, X.; Guan, X.; Zheng, D.; Tian, W.; Li, C.; Li, C.; Yan, M.; Yao, Y. Construction of interfacial engineering on CoP nanowire arrays with CoFe-LDH nanosheets for enhanced oxygen evolution reaction. *FlatChem* **2021**, *26*, 100225. [[CrossRef](#)]
157. Li, W.; Chen, S.; Zhong, M.; Wang, C.; Lu, X. Synergistic coupling of NiFe layered double hydroxides with Co-C nanofibers for high-efficiency oxygen evolution reaction. *Chem. Eng. J.* **2021**, *415*, 128879. [[CrossRef](#)]
158. Duan, H.; Chen, Z.; Xu, N.; Qiao, S.; Chen, G.; Li, D.; Deng, W.; Jiang, F. Non-stoichiometric NiOx nanocrystals for highly efficient electrocatalytic oxygen evolution reaction. *J. Electroanal. Chem.* **2021**, 114966. [[CrossRef](#)]
159. Zhang, S.; Wei, N.; Yao, Z.; Zhao, X.; Du, M.; Zhou, Q. Oxygen vacancy-based ultrathin Co_3O_4 nanosheets as a high-efficiency electrocatalyst for oxygen evolution reaction. *Int. J. Hydrog. Energy* **2021**, *46*, 5286–5295. [[CrossRef](#)]
160. Shinde, P.; Rout, C.S.; Late, D.; Tyagi, P.K.; Singh, M.K. Optimized performance of nickel in crystal-layered arrangement of $\text{NiFe}_2\text{O}_4/\text{rGO}$ hybrid for high-performance oxygen evolution reaction. *Int. J. Hydrog. Energy* **2021**, *46*, 2617–2629. [[CrossRef](#)]
161. Zhang, Z.; Xu, Y.; Wu, M.; Luo, B.; Hao, J.; Shi, W. Homogeneously dispersed cobalt/iron electrocatalysts with oxygen vacancies and favorable hydrophilicity for efficient oxygen evolution reaction. *Int. J. Hydrog. Energy* **2021**. [[CrossRef](#)]
162. Tang, J.; Xu, J.L.; Ye, Z.G.; Li, X.B.; Luo, J.M. Microwave sintered porous CoCrFeNiMo high entropy alloy as an efficient electrocatalyst for alkaline oxygen evolution reaction. *J. Mater. Sci. Technol.* **2021**, *79*, 171–177. [[CrossRef](#)]
163. Kim, J.; Lee, J.; Liu, C.; Pandey, S.; Woo Joo, S.; Son, N.; Kang, M. Achieving a long-term stability by self-redox property between Fe and Mn ions in the iron-manganese spinel structured electrode in oxygen evolution reaction. *Appl. Surf. Sci.* **2021**, *546*, 149124. [[CrossRef](#)]
164. Li, D.; Liu, C.; Ma, W.; Xu, S.; Lu, Y.; Wei, W.; Zhu, J.; Jiang, D. Fe-doped NiCoP/Prussian blue analog hollow nanocubes as an efficient electrocatalyst for oxygen evolution reaction. *Electrochim. Acta* **2021**, *367*, 137492. [[CrossRef](#)]
165. Yu, C.; Cao, Z.; Chen, S.; Wang, S.; Zhong, H.; Ma, X. In situ selenylation of molybdate ion intercalated Co-Al layered double hydroxide for high-performance electrocatalytic oxygen evolution reaction. *J. Taiwan Inst. Chem. Eng.* **2021**. [[CrossRef](#)]
166. Ma, F.; Wu, Q.; Liu, M.; Zheng, L.; Tong, F.; Wang, Z.; Wang, P.; Liu, Y.; Cheng, H.; Dai, Y.; et al. Surface Fluorination Engineering of NiFe Prussian Blue Analogue Derivatives for Highly Efficient Oxygen Evolution Reaction. *ACS Appl. Mater. Interfaces* **2021**. [[CrossRef](#)] [[PubMed](#)]
167. Xing, D.; Zhou, P.; Liu, Y.; Wang, Z.; Wang, P.; Zheng, Z.; Dai, Y.; Whangbo, M.H.; Huang, B. Atomically dispersed cobalt-based species anchored on polythiophene as an efficient electrocatalyst for oxygen evolution reaction. *Appl. Surf. Sci.* **2021**, *545*, 148943. [[CrossRef](#)]
168. Dong, Q.; Shuai, C.; Mo, Z.; Liu, N.; Liu, G.; Wang, J.; Pei, H.; Jia, Q.; Liu, W.; Guo, X. CeO_2 nanoparticles@ NiFe-LDH nanosheet heterostructure as electrocatalysts for oxygen evolution reaction. *J. Solid State Chem.* **2021**, *296*, 121967. [[CrossRef](#)]

169. Huang, C.; Zhong, Y.; Chen, J.; Li, J.; Zhang, W.; Zhou, J.; Zhang, Y.; Yu, L.; Yu, Y. Fe induced nanostructure reorganization and electronic structure modulation over CoNi (oxy)hydroxide nanorod arrays for boosting oxygen evolution reaction. *Chem. Eng. J.* **2021**, *403*, 126304. [[CrossRef](#)]
170. Ganesan, V.; Son, J.-H.; Kim, J. CoP₂/Fe-CoP₂ yolk-shell nanoboxes as efficient electrocatalysts for oxygen evolution reaction. *Nanoscale* **2021**. [[CrossRef](#)] [[PubMed](#)]
171. Song, Y.; Zhao, X.; Liu, Z.-H. Surface selenium doped hollow heterostructure/defects Co-Fe sulfide nanoboxes for enhancing oxygen evolution reaction and supercapacitors. *Electrochim. Acta* **2021**, *374*, 137962. [[CrossRef](#)]
172. Sadaqat, M.; Manzoor, S.; Nisar, L.; Hassan, A.; Tyagi, D.; Shah, J.H.; Ashiq, M.N.; Joya, K.S.; Alshahrani, T.; Najam-ul-Haq, M. Iron doped nickel ditelluride hierarchical nanoflakes arrays directly grown on nickel foam as robust electrodes for oxygen evolution reaction. *Electrochim. Acta* **2021**, *371*, 137830. [[CrossRef](#)]
173. Dong, W.; Zhou, H.; Mao, B.; Zhang, Z.; Liu, Y.; Liu, Y.; Li, F.; Zhang, D.; Zhang, D.; Shi, W. Efficient MOF-derived V-Ni₃S₂ nanosheet arrays for electrocatalytic overall water splitting in alkali. *Int. J. Hydrog. Energy* **2021**. [[CrossRef](#)]
174. Yuan, C.-Z.; Sun, Z.-T.; Jiang, Y.-F.; Yang, Z.-K.; Jiang, N.; Zhao, Z.-W.; Qazi, U.Y.; Zhang, W.-H.; Xu, A.-W. One-Step in Situ Growth of Iron-Nickel Sulfide Nanosheets on FeNi Alloy Foils: High-Performance and Self-Supported Electrodes for Water Oxidation. *Small* **2017**, *13*, 1604161. [[CrossRef](#)]
175. Wu, A.; Xie, Y.; Ma, H.; Tian, C.; Gu, Y.; Yan, H.; Zhang, X.; Yang, G.; Fu, H. Integrating the active OER and HER components as the heterostructures for the efficient overall water splitting. *Nano Energy* **2018**, *44*, 353–363. [[CrossRef](#)]
176. Zhang, L.; Wang, X.; Li, A.; Zheng, X.; Peng, L.; Huang, J.; Deng, Z.; Chen, H.; Wei, Z. Rational construction of macroporous CoFeP triangular plate arrays from bimetal-organic frameworks as high-performance overall water-splitting catalysts. *J. Mater. Chem. A* **2019**, *7*, 17529–17535. [[CrossRef](#)]
177. Sun, H.; Min, Y.; Yang, W.; Lian, Y.; Lin, L.; Feng, K.; Deng, Z.; Chen, M.; Zhong, J.; Xu, L.; et al. Morphological and Electronic Tuning of Ni₂P through Iron Doping toward Highly Efficient Water Splitting. *ACS Catal.* **2019**, *9*, 8882–8892. [[CrossRef](#)]
178. Wang, J.; Yang, W.; Liu, J. CoP₂ nanoparticles on reduced graphene oxide sheets as a super-efficient bifunctional electrocatalyst for full water splitting. *J. Mater. Chem. A* **2016**, *4*, 4686–4690. [[CrossRef](#)]
179. Ming, F.; Liang, H.; Shi, H.; Xu, X.; Mei, G.; Wang, Z. MOF-derived Co-doped nickel selenide/C electrocatalysts supported on Ni foam for overall water splitting. *J. Mater. Chem. A* **2016**, *4*, 15148–15155. [[CrossRef](#)]
180. Lin, J.; Wang, P.; Wang, H.; Li, C.; Si, X.; Qi, J.; Cao, J.; Zhong, Z.; Fei, W.; Feng, J. Defect-Rich Heterogeneous MoS₂/NiS₂ Nanosheets Electrocatalysts for Efficient Overall Water Splitting. *Adv. Sci.* **2019**, *6*, 1900246. [[CrossRef](#)]
181. Qin, Q.; Chen, L.; Wei, T.; Liu, X. MoS₂/NiS Yolk-Shell Microsphere-Based Electrodes for Overall Water Splitting and Asymmetric Supercapacitor. *Small* **2019**, *15*, 1803639. [[CrossRef](#)] [[PubMed](#)]
182. Li, N.; Zhang, Y.; Jia, M.; Lv, X.; Li, X.; Li, R.; Ding, X.; Zheng, Y.Z.; Tao, X. 1T/2H MoSe₂-on-MXene heterostructure as bifunctional electrocatalyst for efficient overall water splitting. *Electrochim. Acta* **2019**, *326*, 134976. [[CrossRef](#)]